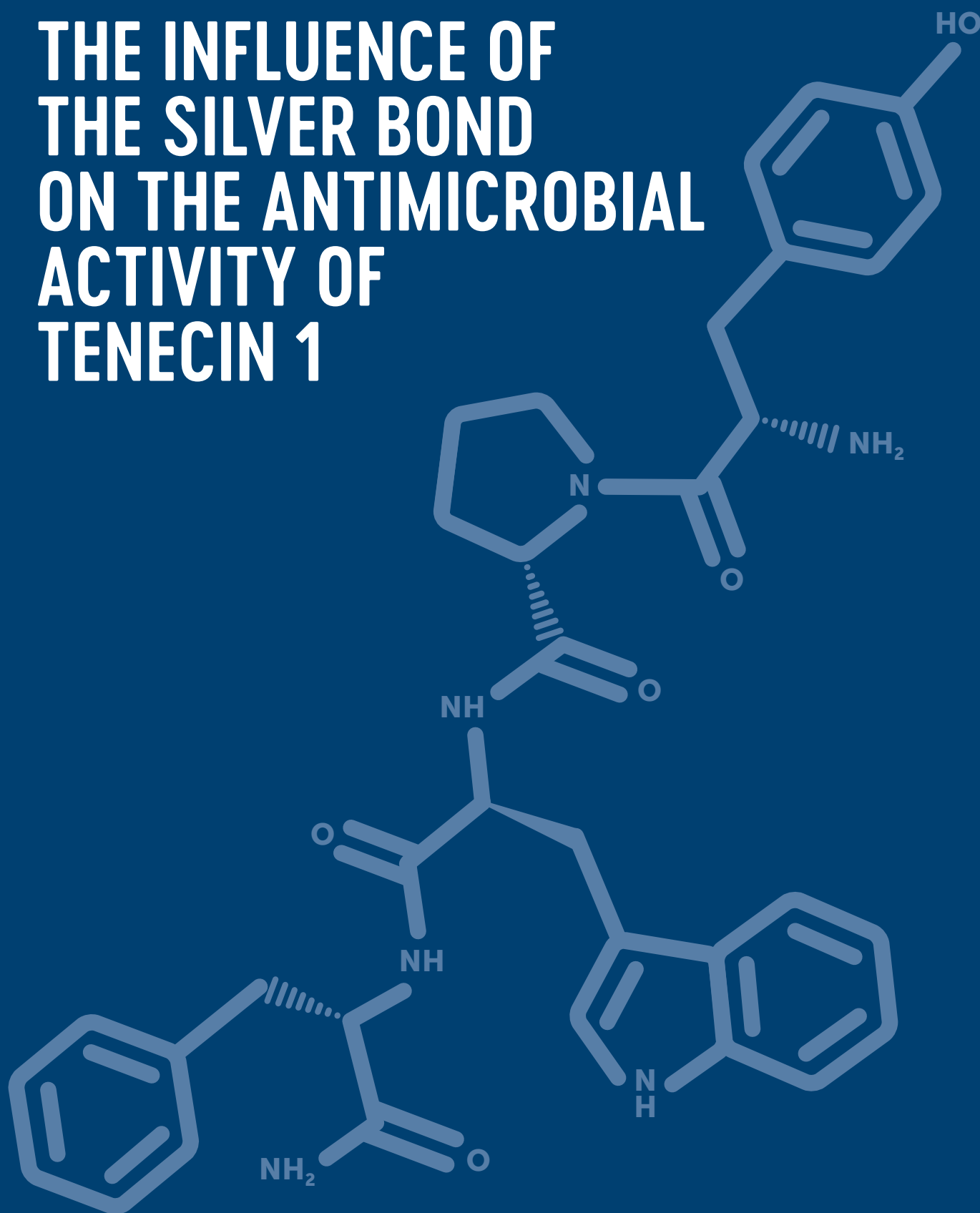# THE INFLUENCE OF THE SILVER BOND ON THE ANTIMICROBIAL ACTIVITY OF TENECIN 1

MASTER'S THESIS BY:
EIMEAR DE BÚRCA
STINE MAAGAARD HANSEN

JUNE 1ST 2023
60 ECTS IN CHEMISTRY AND
MEDICINAL BIOLOGY

SUPERVISORS:
ASSOCIATE PROFESSOR LOTTE JELSBAK
ASSOCIATE PROFESSOR FREDERIK DINESS

RUC | DEPARTMENT OF NATURAL SCIENCE AND ENVIRONMENT | ROSKILDE UNIVERSITY

Table of contents

ABSTRACT

Background: The rapid development of antibiotic resistance towards traditionally used antibiotics has become an increasing problem globally and therefore novel treatment options are currently in the spotlight. Antimicrobial peptides could be a possible solution to this problem, and the optimisation of these peptides is already being investigated. However, other methods may be needed to stabilise their structures before they can be used as therapeutics.

Objective: The objective of this thesis is to investigate whether the antimicrobial activity of the derivatives based on the alpha-helical region within Tenecin 1 against *Staphylococcus aureus* will improve following the addition of silver.

Method: The investigation is based on the analysis of newly provided data from HPLC, LC-MS, CD, minimum inhibitory concentration, biofilm, and haemolysis assays.

Results: The CD-spectra showed a variation of results. Based on the CD results, peptide **AC** w. Ag^+, **4c$^+$** w. Ag^+ and **4c$^+$n$^+$** w. Ag^+ showed great potential in terms of adopting an alpha-helical structure. The MIC-values for all peptides without Ag^+ showed no antimicrobial potential, whilst all peptides with Ag^+ added showed promising results. The peptides showed no significant activity against *Staphylococcus aureus* biofilms, and likewise, they did not show toxicity towards human red blood cells.

Conclusion: Several criteria must be met before the peptides can be used as therapeutic drugs. Certain peptides (**AC**, **4c$^+$** and **4c$^+$n$^+$**) investigated in this thesis exhibit potential in terms of their structural changes following the addition of Ag^+, and likewise, they had a low MIC-value. However, it is unbeknown to which extent free Ag^+-ions have affected the results, and therefore more in-depth experiments are necessary. However, it can be concluded that binding of Ag^+-ions occurs for other peptides besides **AC**, and that this exhibits potential, especially for the peptides with additional charges (**4c$^+$** and **4c$^+$n$^+$**).

Key words: AMP, antibacterial activity, antimicrobial peptide, biofilm, CD, haemolysis, HPLC, LC-MS, MIC, potential drug, structure, Tenecin 1, Tenecin 1 derivatives, treatment.

RESUMÉ

Baggrund: Den tiltagende udvikling af antibiotikaresistens overfor traditionelt anvendt antibiotika er blevet et stigende problem globalt, og grundet dette er nye behandlingsformer i søgelyset. Antimikrobielle peptider kan være en mulig løsning på denne problematik, og optimering af disse peptider er allerede ved at blive undersøgt. Det kan være nødvendigt at tage andre fremgangsmåder i brug for at stabilisere peptidernes strukturer, hvis de skal bruges som fremtidige terapeutiske midler.

Formål: Formålet med dette speciale er derfor at undersøge, hvorvidt den antimikrobielle aktivitet af derivater, der er baseret på den alfa-helikale region af Tenecin 1 mod *Staphylococcus aureus*, vil blive forbedret efter tilsætningen af sølv.

Metode: Undersøgelserne er baseret på analyse af nye data fra HPLC, LC-MS, CD, minimum inhiberende koncentration, biofilm-og hæmolyse forsøg.

Resultater: CD-spektrene viste forskellige resultater, hvor resultaterne fra peptid **AC** m. Ag^+, **4c⁺** m. Ag^+ og **4c⁺n⁺** m. Ag^+ viste et stort potentiale i forhold til at adoptere en alfa-helikal struktur. MIC-værdierne for alle peptider uden tilsat Ag^+ viste intet antimikrobielt potentiale, hvorimod alle peptider med tilsat Ag^+ viste lovende resultater. Derudover viste peptiderne ingen signifikant aktivitet overfor *Staphylococcus aureus* biofilm, og ligeledes viste de ingen toksicitet mod humane røde blodceller.

Konklusion: Flere kriterier skal imødekommes før antimikrobielle peptider kan anvendes som terapeutiske lægemidler. Visse peptider (**AC, 4c⁺** og **4c⁺n⁺**) undersøgt i denne afhandling udviste potentiale i form af deres strukturelle ændringer efter tilsætning af Ag^+, og samtidig havde de en lav MIC-værdi. Det er dog uvist, i hvilket omfang de frie Ag^+-ioner har påvirket resultaterne, og derfor er flere dybdegående eksperimenter nødvendige at udføre. Det kan dog konkluderes, at binding af Ag^+-ioner forekommer hos andre peptider end **AC**, og at dette udviser potentiale i forhold til udvikling af fremtidige lægemidler. Derudover kan det konkluderes, at der er potentiale for peptiderne med ekstra ladninger (**4c⁺** og **4c⁺n⁺**).

Nøgleord: AMP, antibakteriel aktivitet, antimikrobielle peptider, behandling, biofilm, CD, fremtidig lægemiddel, HPLC, hæmolyse, LC-MS, MIC, struktur, Tenecin 1, Tenecin 1 derivater.

PREFACE AND ACKNOWLEDGEMENT

This thesis is the result of a 60 ECTS interdisciplinary master's project combining chemistry and medicinal biology. All laboratory work was carried out by Eimear de Búrca and Stine Maagaard Hansen at the facilities of the Department of Science and Environment at Roskilde University, Denmark, during the period from August 2022 to June 2023. The thesis has been divided into the primary report itself and the appendix, which can be found online on Digital Eksamen as a separate document (56 pages).

We would like to express our gratitude to our chemistry supervisor Associate Professor Frederik Diness and our biology supervisor Associate Professor Lotte Jelsbak for their guidance throughout the course of our thesis. Furthermore, we would like to thank Niklas Henrik Fischer (postdoc) and Jacob Tofte (PhD-student) for their theoretical and practical guidance in chemistry and biology, respectively. Lastly, we would like to thank our laboratory technicians, Anette Christensen, Eva Karlsen and Rosa Jersie-Christensen, for guiding us in the laboratory.

LIST OF ABBREVIATIONS

Abbreviation	Expansion
AA	Amino acid
Ag^+	Silver
$AgNO_3$	Silver nitrate
AGR	Accessory gene regulator
AMP	Antimicrobial peptide
AMR	Antimicrobial resistance
ATP	Adenosine triphosphate
Boc	Tert-butoxycarbonyl
CD	Circular dichroism
CV	Crystal Violet
CWA	Cell wall-anchored
DMF	*N,N*-dimethylformamide
DTDP	4,4'- dithiodipyridine
ECM	Extracellular matrix
eDNA	Extracellular DNA
EDTA	Ethylenediaminetetraacetic acid
EPS	Extracellular polymeric substances
Equiv.	Equivalents
EU	European Union
Fmoc	Fluorenylmethoxycarbonyl
GN	Gram negative
GP	Gram positive
HPLC	High Performance Liquid Chromatography
HSAB	Hard-soft-acid-base
LB	Lysogeny broth
LC-MS	Liquid chromatography–mass spectrometry
LD_{50}	Lethal dose 50
LPS	Lipopolysaccharide

MeCN	Methyl-cyanide/Acetonitrile
MHB	Mueller-Hinton broth
MIC	Minimum inhibitory concentration
MOA	Mode of action
MRSA	Methicillin-resistant *Staphylococcus aureus*
MSCRAMM	Microbial surface components recognising adhesive matrix molecules
MW	Molecular weight
nm	Nanometre
NMR	Nuclear magnetic resonance
OD	Optical density
ON	Overnight
Pbf	Pentamethyldihydrobenzofuran-5-sulfonyl
pm	Picometer
PSM	Phenol soluble modulin
RBC	Red blood cell
rpm	Rounds per minutes
SA	*Staphylococcus aureus*
SPPS	Solid-phase peptide synthesis
TFA	Trifluoroacetic acid
TFE	2,2,2- trifluoroethanol
TIPS	Tri-isopropyl silane
TOF	Time of flight
UV-vis	Ultraviolet–visible

FIGURES, GRAPHS AND TABLES

Figures:

Graphs:

Tables:

INTRODUCTION

The rapid development of antimicrobial resistance (AMR) poses a great threat to global public health and has become a major challenge for the healthcare community. The phenomenon refers to the ability of microorganisms to resist the effects of antimicrobial agents that were once effective in treating infections caused by them[1–6]. The rise of AMR has led to an increase in the morbidity, mortality, and healthcare costs associated with infectious diseases, making it a critical issue that requires immediate attention and action[7]. Therefore, alternative therapeutic agents are in the spotlight within the scientific field[4,5,8,9].

Agents that have exhibited great potential and could become the next generation of antibiotics are antimicrobial peptides (AMPs)[4]. AMPs were first discovered and identified during the 1980's and occur naturally within the innate immune system of all living organisms[8]. Their antimicrobial activity depends on multiple factors including amino acid (AA) sequence, cationicity, hydrophobicity and amphipathicity[10].

In 2005, Ahn and co-workers documented that Tenecin 1 (an AMP) showed great antimicrobial activity against various microorganisms, of which the highest was observed for Staphylococcus aureus (SA). Likewise, four variations of the sequences corresponding to the alpha-helical region of Tenecin 1 exhibited antimicrobial activity of which sequence **4** showed the greatest potential against SA. Common for all the sequences is that they possess two cysteine units in positions *i,i+4*. However, they only adopt alpha helicity under membrane mimicked conditions. Despite their potential as therapeutic agents, the antimicrobial activity of the four sequences can be further optimised through stabilisation of their alpha-helical region[11].

In 2022, Diness and co-workers demonstrated that the addition of silver-ions (Ag$^+$) to a peptide containing two cysteine units in positions *i,i+4* induced a change in secondary structure from random coil to alpha-helix[12]. Ag$^+$ has previously been used for medicinal purposes such as treatment of burn wounds and prevention of biofilm formation in catheters and heart valves[13,14]. On the downside, Ag$^+$-based compounds have led to the development of resistance in various bacterial species[13,15], and moreover, Ag$^+$ has shown toxicity in high doses (LD$_{50}$ 800 mg of silver/kg of body weight/day in rabbits)[16,17].

Based upon the discoveries by Ahn and Diness, the four derivatives corresponding to the alpha-helical region of Tenecin 1 could possibly be optimised by the addition of Ag^+. This could in turn improve their antimicrobial activity against SA and eventually prevent formation of biofilm.

1. BACKGROUND

1.1 Peptide/protein structure

Peptides are short proteins usually consisting of fewer than 50 AAs[9], and four different levels of complexity are used to describe the structures of peptides and proteins: the primary, secondary, tertiary, and quaternary structures. The primary structure is the sequence of AAs used to build the peptide. The secondary structure refers to the stable arrangement of AA units that gives rise to structural patterns such as alpha-helixes and beta-sheets, and the tertiary structures describe all aspects of the three-dimensional folding of a polypeptide. When a protein consists of two or more polypeptides, this arrangement is referred to as the quaternary structure. In the following section, the focus will mainly be on the primary and secondary structures of proteins and peptides[18–20].

Primary structure

The primary structure of a peptide consists of the sequence of AAs that constitute the protein itself. All the AAs have a central carbon atom, which is called the alpha carbon (**figure 1**). Four functional groups are bound to the alpha carbon, which includes a hydrogen, an amino group, a carboxyl group, and a sidechain, that is often called the R-group (**figure 1**)[18,20].
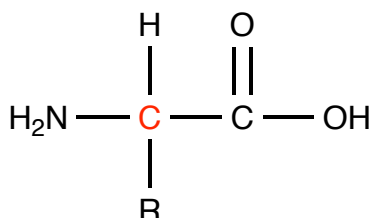
Figure 1: An illustration of the general structure of an amino acid[18]

The figure illustrates the general structure of an AA with its alpha carbon highlighted in red. The four functional groups within an AA are an amino group, a carboxyl group, a hydrogen, and a sidechain (annotated with R)[18]. The illustration was prepared with ChemDraw.

Different AAs have different properties and can be divided into sub-categories based upon their chemical properties. The R-group is conclusive in dividing these AAs into four groups according to polarity and furthermore, the overall charge of a protein is primarily due to the R-group, as the alpha-amino- and carboxyl groups form the peptide bond and therefore do not affect the charge of the peptide[18,20].

- Non-polar, aliphatic R-groups; These sidechains are solely made up of hydrocarbon chains, making this group non-polar and reasonably hydrophobic. Furthermore, these AA tend to "cluster" together inside a protein thus stabilising the structure through hydrophobic effects[18,20].

- Polar, uncharged R-groups; The polar uncharged R-groups interact with either water molecules or atoms within other side chains. This interaction happens through hydrogen bonds, where a donor hydrogen atom, which is covalently bound to an electronegative atom, and an acceptor atom, typically with a lone pair of electrons, interact, e.g., when two serine units lay within proximity[18,20].

- Polar, charged R-groups; The AAs lysine and arginine are basic since they are positively charged at pH 7, whereas the AAs asparagine and glutamic acid are acidic as they have a negative charge at pH 7. Furthermore, charged R-groups can form hydrogen bonds and ionic interactions with AAs of opposite charge[18,20].

- Non-polar, aromatic R-groups: The aromatic R-groups help make an AA hydrophobic, affecting the protein's polarity and hydrophobic effect[18,20].

A polypeptide chain is made up of a sequence of AAs, where a covalent bond is formed between two AA, which is called a peptide bond. A condensation reaction creates the peptide bond, i.e., a reaction where water is removed as the alpha-carbon carboxyl group of one AA reacts with the alpha-carbon amino group of another AA. This reaction results in a polypeptide chain having an amino terminus (*N*-terminus) and a carboxyl terminus (*C*-terminus)[20,21]. The alpha carbons in the two AAs within a polypeptide chain are separated by three covalent bonds $C_{alpha} - C - N - C_{alpha}$, where $C - N$ is the link in the peptide bond that connects the two AAs. However, all four atoms contribute to the bond and form the polypeptide backbone (**figure 2**)[20].
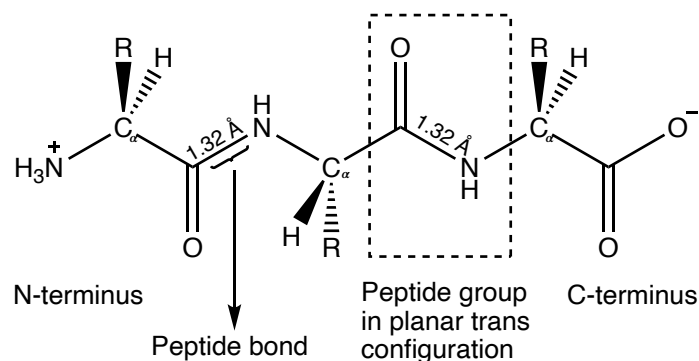
Figure 2: An illustration of the peptide backbone[19,20]

The figure illustrates the conformation of the peptide backbone including its plane. Furthermore, the length of the C – N bond (also known as a peptide bond) is shown and has an average length of 1.32 Å, which is shorter than a usual single bond[19,20]. The illustration was prepared with ChemDraw.

In general, single bonds typically allow for free rotation between the participating atoms, but this does not apply regarding peptide bonds. This is valid because it has been investigated that the four atoms in the peptide backbone lie within the same plane. Likewise, it has been found that the length of the C – N bond is 1.32 Å, which is shorter than a typical single bond of 1.49 Å and corresponds more closely to a C = N bond of 1.27 Å. This is due to resonance, where carboxyl O and amide N shared electrons form a partial double bond (**figure 3**)[20].
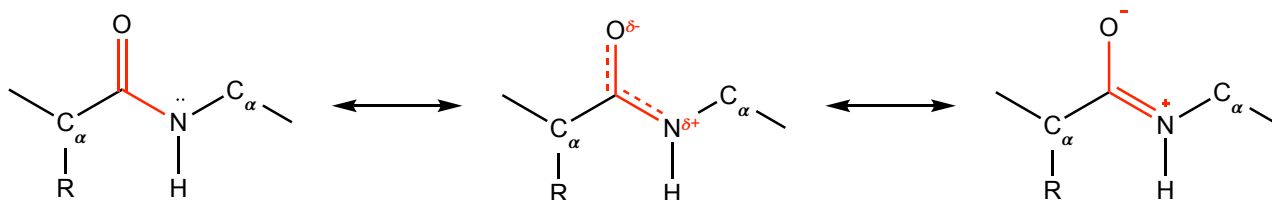
Figure 3: Resonance structure for the peptide bond[20]

The figure illustrates the resonance structure that occurs within a peptide bond[20]. The illustration was prepared with ChemDraw.

This further supports the fact that there is no free rotation around a double bond and a partial double bond gives two possible configurations, either *cis-* or *trans* isomers. Furthermore, it is common that in peptide bonds, the *trans* isomer is preferred over the *cis* isomer. The *trans* isomer is where the two alpha carbons lie on opposite sides of the peptide bond, and the same applies to carbonyl O and amide H (**figure 4**)[20].

A) Trans   B) Cis
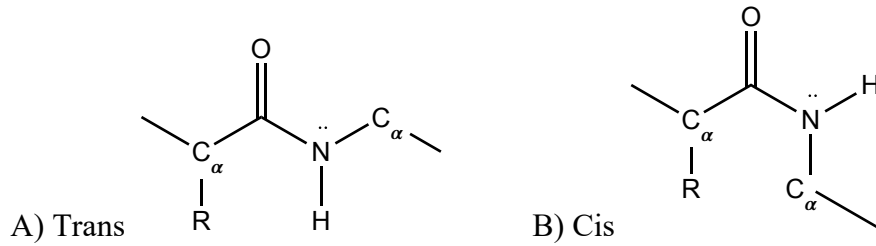
Figure 4: An illustration of trans and cis isomers within a peptide[20]

The figure illustrates two different isomers (trans and cis) of the same peptide[20]. The illustration was prepared with ChemDraw.

The $C_{alpha} - C$ and $N - C_{alpha}$ bonds can rotate freely (**figure 4, A**), however, there are limitations to the rotation as the bulky side groups can obstruct. Therefore, it can also be said that a peptide bond consists of a series of rigid planes. Furthermore, the peptide bonds are relatively strong, and the known half-life is about seven years under intracellular conditions[18,20].

Secondary structure

The secondary structure describes the repeating elements in a protein or peptide where hydrogen bonds are formed between the polar atoms of the peptide backbone. The most common secondary structures are the alpha-helix, which is typically between $10 - 15$ units long, and the beta-sheet, which is between $3 - 10$ units long. A typical protein usually contains approximately $\frac{1}{3}$ alpha-helix and $\frac{1}{3}$ beta-sheet, but deviations occur. Segments of proteins that neither consist of alpha nor beta usually consist of loops and turns[19,20]. An alpha-helix consists of 3.6 AA per turn; a complete turn is usually 5.4 Å (1.5 Å per unit) long with the R-groups pointing out from the helix. The helical turn is created by hydrogen on amide N forming a hydrogen bond with carbonyl O on the 4th AA units towards the *N*-terminus[20]. Furthermore, an electric dipole is created by all the alpha-helix amide bond dipoles pointing in the same direction, which results in a partial positive charge on the *N*-terminus and a partial negative charge on the *C*-terminus (**figure 5**)[20,22].
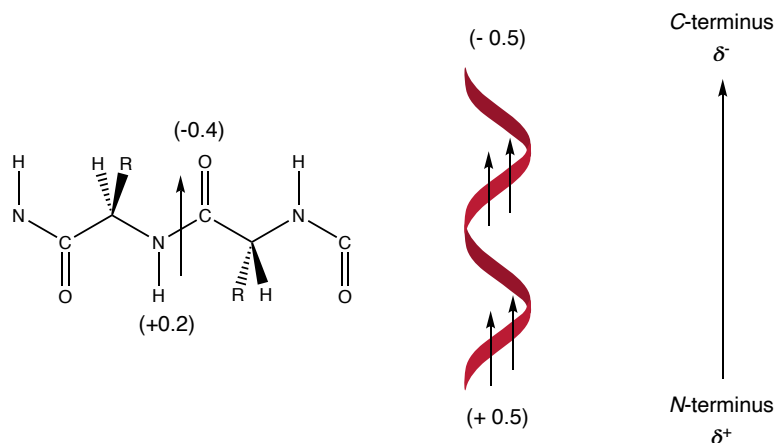
Figure 5: An illustration of the dipole moment within an alpha-helix[22]

The figure illustrates the dipole moment that occurs within an alpha-helix, where the N-terminus is partially positively charged (+0.5) and the C-terminus is partially negatively charged (-0.5)[22]. The illustration was prepared with ChemDraw.

Furthermore, some general guidelines make it possible to predict the likelihood of alpha-helicity based on the AA sequence. For example, contiguous stretches of AA units with long or bulky R-groups cannot come close enough together to form an alpha-helix. Likewise, polar sidechains can form hydrogen bonds to the peptide backbone, resulting in destabilisation of the alpha-helix. Due to this, AAs, such as serine, asparagine, aspartate, and threonine, are seldom found within an alpha-helix. Furthermore, R-groups with the same charge can repel each other and thereby also destabilise the alpha-helix[20].

However, there are also specific arrangements of AAs which can stabilise an alpha-helix, e.g., sidechains separated by four AA units stacked on top of each other in a helix. Likewise, differently charged R-groups that are close to each other can attract the opposite charge and form ion pairs, which can also stabilise the alpha-helix. Additionally, aromatic sidechains separated by four units can also form $\pi - \pi$ interactions, which also contributes to stabilisation[20]. In addition to the mentioned guidelines, graphical presentations of the supposed alpha-helical regions within a peptide can be visualised by two-dimensional projections called helical wheels which illustrates where the hydrophobic regions are located[23].

On the other hand, a beta-sheet usually does not occur alone. To form a so-called beta-sheet, several segments need to be arranged side-by-side, and thereby, a beta-sheet consists of a minimum of two beta strands. Similar to an alpha-helix, a beta-sheet is formed by hydrogen bonds between backbone

amide and carbonyl groups. Furthermore, the peptide bonds in a beta-sheet are arranged with a distance of 3.5 Å per unit. To prevent interactions between the different R-groups of adjacent AAs, the R-groups lie on opposite sides of the sheet[20].

Tertiary and Quaternary structures

In contrast to the primary and secondary structure, the tertiary structure of a protein or peptide describes the different secondary structures, loops, and turns connecting them and gives an overall three-dimensional overview of the structure. Furthermore, the quaternary structure describes the connection between the different polypeptide chains[20].

1.2 Antimicrobial peptides

AMPs, also called host defence peptides, are produced by several different organisms including bacteria, plants, insects, and humans. The production of AMPs is part of the innate immune system and functions as a defence mechanism. The primary role of AMPs is to protect the host by killing invading pathogenic organisms[24–26]. Overall, AMPs exhibit antimicrobial activity against bacteria, fungi, parasites, and viruses. However, the effect of the host defence system may differ between different species and sites within a particular organism[24,26].

AMPs have different advantages and disadvantages. The advantages are many; among other things, AMPs are broad-spectrum in terms of activity, they kill the bacteria quickly, and they should not develop resistance as easily in comparison to traditional antibiotics due to their different mode of action (MOA)[1,3,26]. The MOA of peptides targets the bacterial membrane, whereas traditional antibiotics targets proteins within the bacteria. This entails that the development of resistance based on gene mutation is less likely for AMPs[8]. However, the disadvantages are essential to overcome, as they include toxicity against eukaryote and a severe haemolytic effect[3]. Furthermore, AMPs can be hydrolysed by proteases, their chemical production can be technically challenging and very expensive[1,26,27]. Several factors must be considered and improved before AMPs will be able to solve the ongoing problem regarding development of AMR[1,3,26].

Properties and characteristics

AMPs have distinct characteristics and similarities, although differences do occur. They are usually very short ranging from a size of 10 – 50 AAs in length, and almost all AMPs are cationic, with a positive charge between +2 and +9[3,5,26–28]. This is due to the amount of the positively charged AAs[3,26,27]. Likewise, many AMPs contain fractions of hydrophobic units due to the content of specific AAs. Generally, half of the AAs in the peptide are hydrophobic. These properties enable the peptide to fold into an amphiphilic secondary structure[3,5,8,26,27]. The amphiphilic structure of the alpha-helical AMPs creates an alpha-helix with one face being hydrophobic and the other face hydrophilic, which contributes to the peptide's MOA and selectivity when attacking the bacteria[3,27]. The number of positive charges is therefore related to the antimicrobial activity, which increases their potential as therapeutic drugs. In contrast, as their hydrophobicity increases so does the haemolytic activity, which decreases their potential as therapeutic drugs[3,26].

Cell wall and plasma membrane of bacteria

To better understand the MOA of AMPs, an understanding of how the bacterial cell wall is structured is essential[2]. Bacteria are generally divided into a Gram-negative (GN) or Gram-positive (GP) sub-category due to the differences in their cell envelope[2,26,29]. Both GN and GP bacteria share several different features in their outer cell structure, but it is especially the cell wall and plasma membranes that are essential for AMPs. The MOA commences on the cell wall where the initial attraction between the AMP and the bacterium starts the whole process, whereas the plasma membrane is the location where the AMPs perform their mechanism and function[1–3,26].

The typical cell wall of a GP bacterium consists of a single thick homogeneous layer of peptidoglycan and many other polymers, such as teichoic acid, where some of the teichoic acids protrude beyond the peptidoglycan layer and contribute to the GP cell wall's negative charge (**figure 6**)[2,26,29,30].
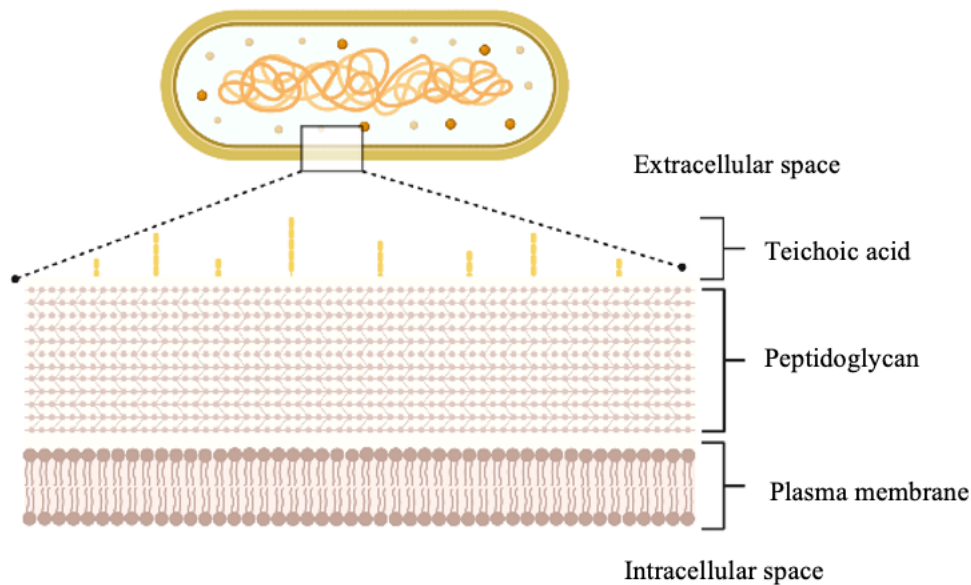
Figure 6: Cell wall and plasma membrane of a Gram-positive bacterium[2,26,29]

The figure illustrates the cell wall and plasma membrane of a GP bacterium consisting of the plasma membrane itself, a thick peptidoglycan layer and a layer of teichoic acids which protrude out towards the extracellular space[2,26,29]. The illustration was prepared with BioRender.

In contrast to the GP cell wall, the GN cell wall is more complex. The GN cell wall consists of a thinner layer of peptidoglycan, but has an additional outer membrane, which covers the peptidoglycan layer. This membrane consists of both an internal and external site, which have different structural properties. The internal site/inner leaflet primarily consists of phosphate lipids, where the external site/outer leaflet consists of lipopolysaccharides (LPS). The negative charge on the GN bacteria is due to the LPS, these molecules are covered by negatively charged phosphate groups, which furthermore can participate in ionic interactions with divalent cations. This matrix results in an electrostatic network with low permeability to most hydrophobic antibiotics (**figure 7**)[2,26,29,30].
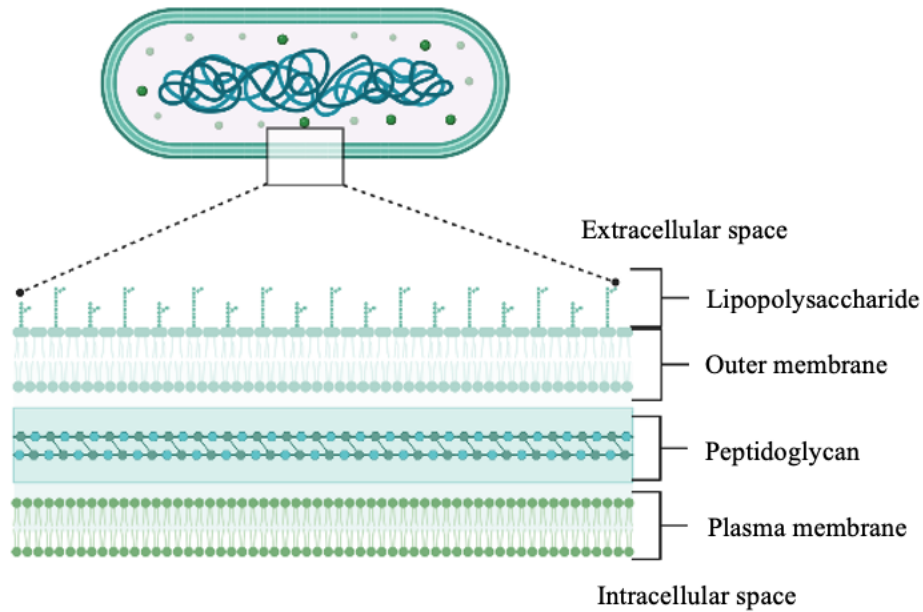
Figure 7: Cell wall and plasma membrane of a Gram-negative bacterium[2,26,29].

The figure illustrates the cell wall and plasma membrane of a GN bacterium consisting of the plasma membrane itself, a thinner layer of peptidoglycan and an outer membrane made up of LPS. Some of the LPS extend beyond the outer membrane and out towards the extracellular space[2,26,29]. The illustration was prepared with BioRender.

The structural and chemical properties of the plasma membrane itself is essential for the AMP's MOA. Based upon that, AMPs can differentiate between multiple organisms and cells[2]. The plasma membrane is dynamic and consists of a lipid bilayer and proteins, both of which can vary in respect to the lipid composition and specific proteins. The lipids in the plasma membrane are amphipathic and organised in a bilayer, where the hydrophilic headgroups point towards the surrounding environment and therefore the cytoplasm. In contrast, the hydrophobic tails point towards each other in the middle of the membrane. The bacterial bilayers' external part contains many lipids with negatively charged phospholipid head groups, which also help to make the surface anionic[26,29].

Mode of action

AMPs' MOA is not fully understood yet, but several different models have been hypothesised. It is also unclear whether the AMPs only attack by one of the hypothesised models or as a combination of several, or even an undiscovered way. However, there is broad agreement about how the first step in the interaction (initial attachment) between the peptide and the target bacterium begins[26,28,31].

The initial attachment starts due to an electrostatic interaction between the cationic peptide (positively charged) and anionic components (negatively charged) of the outer bacterial envelope, e.g., the phosphate groups in LPS in GN bacteria and teichoic acids on the surface of GP bacteria[1,2,26].

Overall, however, the various mechanisms can be divided into two; the models that focus on membrane-disruption and those that focus on non-membrane targeting, i.e., intracellular targets, the latter being better understood[26,28,31]. The membrane-targeting models focus on an extracellular attack and can be further divided into three hypothesised models: The toroidal pore model, the barrel-stave model, and the carpet model (**figure 8**). All these models focus on disrupting or destroying the bacterial membrane itself, which leads to loss of membrane potential, rapid release of intracellular components and membrane lysis, all of which result in cell death[1,26,28,31].
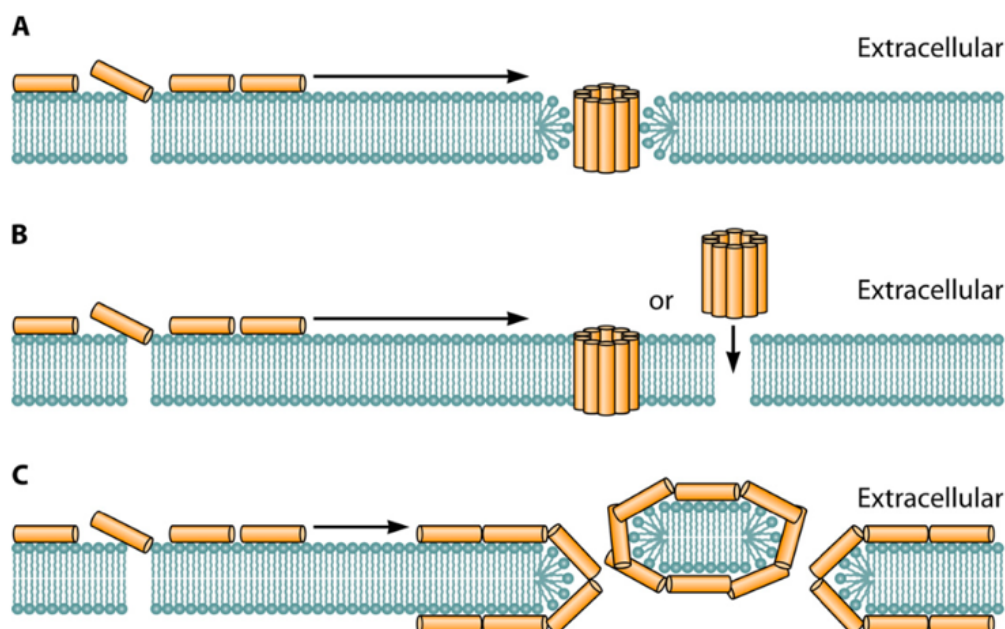
Figure 8: Three hypothesised models for the mode of action of AMPs[31]

The figure illustrates the three types of mechanisms of action of AMPs. Figure A illustrates the toroidal pore model, figure B illustrates the barrel-stave model, and lastly figure C illustrates the carpet model[31].

In the toroidal pore model, the AMPs are embedded vertically into the bacterial cell membrane, causing the phospholipid parts in both the outer and inner membrane to fold inwards. The fold causes the formation of a channel or a so-called pore through the membrane which is covered by several peptide-units. The hydrophilic lipid headgroups in the bacterial membrane are thus closely connected to the hydrophobic face of the AMPs (**figure 8, A**)[1,26,28,31].

The barrel-stave model also focuses on an interaction with the membrane itself like the toroidal pore model. But this model assumes a different way in which the peptide is inserted. The barrel-stave model hypothesised a form of perpendicular insertion into the phospholipid bilayer, resulting in a pore through the membrane where the peptides are parallel to the phospholipids in the plasma membrane. This thus creates a pore where the peptides are in line with the hydrophobic site and the cavity within the pore hydrophilic (**figure 8, B**)[1,26,28,31].

The carpet model differs significantly from the other assumed models, as it hypothesises a horizontal accumulation of peptides on the bacterial membrane. The hypothesised model assumes that this accumulation on the surface leads to a rigidity or tension on the plasma membrane, which will result in various regions of weakness of the membrane and possibly a breakdown of the bilayer in these areas (**figure 8, C**)[1,26,28,31].

In the other sub-category, non-membrane targeting models, the focal point is intracellularly, and the primary focus is on an inhibitory function in contrast to the membrane targeting models, where disintegration of the membrane is the focus. Peptides that function in this manner have different methods of attack and inhibit various synthetic pathways within the bacterial cell, thereby weakening the bacteria. However, since this type of AMP does not destroy the plasma membrane, it is believed that the route through it is via direct penetration or endocytosis. When the AMP is inside the bacterial cell, there are different ways it can identify and attack its target. One can generally divide this type of attack into four different areas which includes inhibition of protein biosynthesis, inhibition of nucleic acid biosynthesis, inhibition of cell division and inhibition of protease activity[26,28,31].

Modification and optimisation

AMPs have shown a great potential to become therapeutic agents, but there are still disadvantages that need to be resolved such as their high haemolytic effect which destroys erythrocytes, expensive costs, and hydrolysis by proteases. However, these factors can be improved by various modifications and designs of the peptides. The primary focal points of the modifications concern the chain length, secondary structure, overall charge, amphiphilicity and hydrophobicity via chemical changes in the sequence. The design of AMPs starts from the naturally occurring AMPs, which are used as a template to identify the chemical properties essential for designing new ones with fewer disadvantages[3,26,28].

1.2.1 Tenecin 1

Tenecin 1 is a cationic AMP produced and secreted by the larvae of *Tenebrio molitor* in response to a bacterial infection[11,32,33]. The peptide consists of 43 AAs of which 6 are cysteine residues and features three intramolecular disulphidebridges[11,33,34].

Ahn and co-workers have documented that Tenecin 1 has shown bactericidal activity towards GP bacteria, such as *S. aureus* (SA), and GN bacteria to a lesser extent. The peptide features a short amphipathic α-helical region at the *N*-terminal followed by an antiparallel β-sheet region at the *C*-terminal. The α-helical and β-sheet regions are stabilised by two disulphide bridges known as a cysteine stabilised α/β-motif. Furthermore, studies have shown that the fragments corresponding to the β-sheet region of the peptide exhibits antimicrobial activity, whereas the α-helical region showed no antimicrobial activity. Despite the lack of antimicrobial activity, the α-helical region of Tenecin 1 resembles other well-known AMPs regarding its amphiphilic structure and hydrophobicity amongst others [11,32,33].

Moreover, Ahn and co-workers have synthetised four derivatives corresponding to the alpha-helical region of Tenecin 1, which showed antimicrobial activity. Additionally, the derivatives express alpha-helicity under conditions meant to mimic the lipid bilayer of bacteria. In contrast, the same alpha-helical region of the peptide adopts a random coiled secondary structure in phosphate-buffered saline (PBS). With a pH of 7.4, PBS is used to mimic the body's physiological conditions [11,33].

1.3 Silver

Silver has been applied for medical purposes as early as 1000 BC [35]. The development of the medical sphere during the 1940's led to the discovery and production of antibiotics – some of which are still in use till this day. Due to the development of bacterial resistance mechanisms towards commonly used antibiotics, the use of silver for medicinal purposes is slowly gaining popularity again and could lead to the development of a novel generation of antibiotics[15].

Ag^+ and silver-based compounds, such as silver nitrate ($AgNO_3$), are well-known for their bacteriostatic and bactericidal effects towards as many as 12 bacterial species[14,35]. It is worth mentioning the antimicrobial activity of $AgNO_3$ which has a minimum inhibitory concentration (MIC)-value of 3 μM towards *E. coli*[36]. During the 19th century, silver in therapeutics was used for the treatment of burn wounds and prevention of biofilm formation in catheters and heart valves[13].

On the downside, Ag^+-based compounds have led to the development of resistance in various bacterial species. Resistance towards Ag^+ is mainly due to the lack of accumulation of Ag^+ within the bacterium. This lack of accumulation is caused by several *sil*-genes, including *sil*E and *sil*F, that are both responsible for driving Ag^+-ions out from within the cell, and over-stimulation of *sil*P and *sil*CBA, that are both responsible for the efflux pumps[37,38].

Coordination of Ag⁺

It has already been established that metal-ions can form complexes with proteins and peptides[39]. Formation of such complexes can influence the secondary structure of the peptide which in turn can alter its biological activity[40]. An example of coordination between metal-ions and peptides in the human body include the *CueR*, that activates the *Cue operon* which regulates metal ion homeostasis in response to elevated cellular levels of group 11 transition metals which includes Cu^+, Ag^+ and Au^+[12,41].

Diness and co-workers have recently shown that alpha-helicity can be induced by the addition and coordination of Ag^+ to selected AA residues within a peptide containing the AA-motif cysteine-X-X-X-cysteine. Their research showed that Ag^+ coordinates to cysteine residues in positions *i,i+4*, which induces alpha-helicity (**figure 9**). The recorded circular dichroism (CD)

spectrum of the peptide prior to the addition of Ag^+ showed a random coiled structure whereas the CD spectrum post addition of Ag^+ showed a significant alpha-helical signal[12].
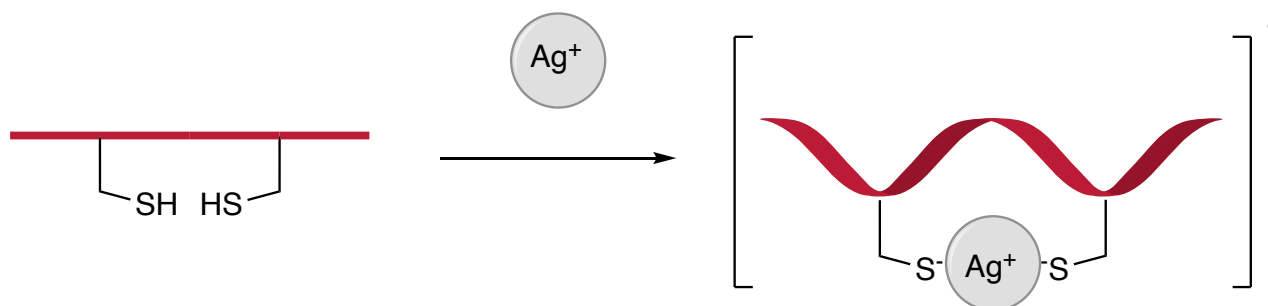
Figure 9: Coordination of Ag$^+$ to thiol groups[12]

The figure illustrates the coordination of silver to thiol groups within a peptide, and its effect on the peptide's secondary structure[12]. The illustration was prepared with ChemDraw.

The alpha-helical structure of peptides and proteins play an important role for their biological function. Sequences of up to 15 AAs corresponding to the alpha-helical region of the peptide are very seldom alpha-helical when isolated from their stabilising environment[42]. Studies performed on alpha-helical regions of other peptides have showed that coordination of metal ions to AA residues containing hetero atoms within the sequence induced an alpha-helical structure[43,44].

Although the exact biological mechanism behind the antimicrobial effect of Ag^+ is not fully understood, several studies confirm that the coordination between Ag^+ and thiol-containing groups in biomolecules within a bacterial species play an important role in its inhibition[45]. It is believed that Ag^+ coordinates with thiol-groups in biomolecules, including DNA, RNA, and proteins, which alters the secondary structure of the molecule thus leading to its inactivation. A study performed by Feng et al. suggests different mechanisms of action on the antimicrobial effect of Ag^+. Firstly, Ag^+ has a denaturing effect on DNA; the DNA condenses and thereby loses its ability to replicate as a response to Ag^+-coordination. Secondly, Ag^+-coordination to biomolecules containing thiol-groups inactivates the proteins produced by the bacterial species. Biological processes that are known to be hindered by the coordination of Ag^+ include adenosine triphosphate (ATP) synthesis and the transportation of potassium within the bacterial cell[45].

The mechanism behind the coordination of Ag^+ to cysteine residues can be explained by using the *hard-soft-acid-base* (HSAB) principle[46]. According to the HSAB principle, the most stable complexes are obtained between acids (electron acceptors) and bases (electron donors) that share

some of the same characteristics such as similar electronegativity, ion radii and polarizability. Acids and bases with low polarizability are classified as hard whereas acids and bases with high polarizability are classified as soft. The polarizability of an atom is determined by factors such as how closely the electrons are bound to the nucleus; closely bound electrons exhibit low polarizability, and the atom is classified as hard whereas loosely bound electrons are highly polarizable making the atom soft. The covalent bond is created between a soft Lewis acid and a soft Lewis base, whereas an ion-bond is created between a hard Lewis acid and a hard Lewis base[45–48].

Cysteine is an AA containing a sulphur atom in its sidechain. The coordination of Ag^+ to the sulphur atom in the cysteine residues can be explained based upon the HSAB principle[45,47]. The soft Lewis acid in the complex is Ag^+ with an electronegativity of 1.93[49] and an ion radius of 126 picometer (pm)[50].

The soft Lewis base in the complex is sulphur whose atomic radius, S^{2-}-ion radius and electronegativity are 103 pm[51], 184 pm[52] and 2.58[49], respectively. Once an atom gains electrons, the anion's size becomes larger than the original atom due to an imbalance between the numbers of protons and electrons, and therefore, the ion radius of S^-- ion must lie between 103 and 184 pm[53,54]. Thereby, a strong covalent bond is formed between the sulphur atom and Ag^+.

1.4 *Staphylococcus aureus* and MRSA

Staphylococcus aureus (SA) is a GP, cocci-shaped, non-motile and non-spore-forming bacterium. The bacterium is found in the environment and in the normal human bacterial flora, typically on the skin and in the nasopharynx. Humans are the primary reservoir for the bacteria, and it is estimated that half of all adults are colonised by SA, while approximately 15 % have the bacteria in the nose. Furthermore, the bacterium is a widespread pathogen in society and hospitals. Usually, SA does not cause infections on healthy, intact skin, however, if the bacterium enters the body or the bloodstream, the bacterium can lead to severe infections, mainly seen in hospitals, such as bacteraemia, infective endocarditis, and toxic shock syndrome[55,56]. In 2019, 119,000 humans suffered from SA bacteraemia (SAB) in the US, of which 20,000 died from the infection[57]. Furthermore, an increasing tendency of SAB has been recorded in Denmark. In 2021, 2,512 cases were registered and over the last 25 years, the fatality rate has been between 17 – 24 %[58].

In addition, the bacteria can form biofilm, which can be found on indwelling medical devices, such as implanted artificial heart valves, catheters, and joint prosthetics. Previously, the bacterium was treated with beta-lactam antibiotics including penicillin and methicillin, however, due to the rise of resistant strains of SA, treatment of infections caused by the bacterium has become extremely challenging[55,56,59].

One of the most prominent resistant strains of the bacteria is methicillin-resistant *Staphylococcus aureus* (MRSA), which causes healthcare- and community-associated infections worldwide. Within the healthcare setting alone, MRSA infections are estimated to affect more than 150,000 patients annually in the European Union (EU). Regardless, treatment methods for MRSA are becoming sparce due to the development of vancomycin-resistant strains. Hence the so-called last resort treatment is in danger [6,60].

1.5 Biofilm

A biofilm aggregate is an extracellular matrix (ECM) produced by community of bacteria. Besides the bacteria, it consists largely of extracellular polymeric substances (EPS) such as polysaccharides, proteins, nucleic acids, and lipids[59,61]. Biofilms are produced by biofilm-producing bacteria, including SA, in aqueous solution, which allows for the microbial cell to adhere to solid surfaces[62]. The mechanisms behind the formation of biofilm vary for each bacterium and depend on different factors such as environmental conditions and features that are specific for the bacterial strain[63]. The biofilm aggregate serves a range of purposes which include increasing the ability of the bacteria to survive in the specific environment and keeping the bacteria in the biofilm within proximity allowing cell-to-cell communication[64].

Although the molecular constituents vary from bacteria to bacteria, the formation of most biofilms occurs in the following steps: *attachment*, *multiplication*, and *dispersal* (**figure 10, A, B and E**). The initial *adhesion* of the free-living bacteria, also known as planktonic bacteria, can occur onto biotic or abiotic surfaces, e.g., the surface of a valve and the surface of a catheter, respectively. In general, planktonic bacterial cells can attach to medical devises in two different ways; the bacterial cell can either adhere to the devise through interactions with the polymer surface of the device or through interactions with human matrix proteins which cover the device. Once the planktonic cells have adhered to a surface, multiplication commences through the production of an ECM. Once the ECM

has been produced, the bacterial cells live in symbiosis with each other. Dispersal occurs when cells and cell-clusters detach from the biofilm, and this step enables cells to spread to other infection sites through the blood and extracellular fluids[59,65].
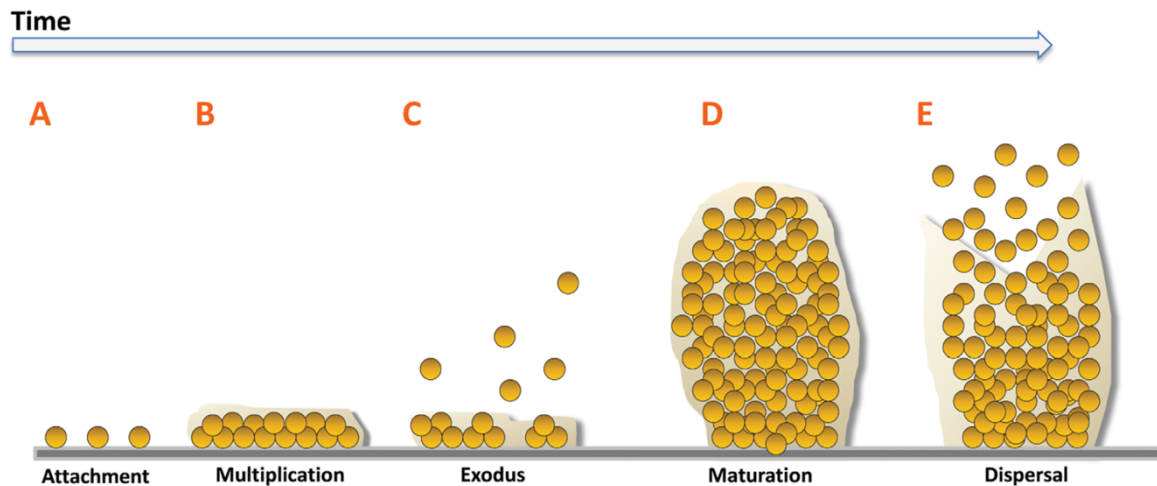
Figure 10: The stages of biofilm formation for **Staphylococcus aureus**[59]

The figure illustrates the five different stages of biofilm formation for SA. Stage A illustrates the initial attachment of planktonic cells followed by stage B, where planktonic cell multiply and an ECM is produced. In stage C, several cells from within the biofilm are released, and in stage D, three-dimensional microcolonies are formed. In the final stage E, detachment of the biofilm occurs allowing the biofilm to spread to other sites of infection[59].

Although its biofilm formation is more complex, planktonic SA can also attach to medical devises in a biotic or abiotic manner. In a biotic fashion, the bacterial cell adheres to the devise through interactions with its polymer surface using a variation of different cell wall-anchored (CWA) proteins known as the microbial surface components recognising adhesive matrix molecules (MSCRAMMs) (**figure 10, A**). In the absence of matrix molecules, SA can attach to abiotic surfaces through different mechanisms including electrostatic and hydrophobic interactions with the charged polystyrene surface. Furthermore, the negatively charged teichoic acids found within GP bacteria, can interact with polystyrene and glass surfaces resulting in attachment, and lastly, autolysin A has been shown to aid in cell attachment to hydrophobic and hydrophilic polystyrene surfaces[59,66].

Once the planktonic cells have adhered to a surface, *multiplication* commences (**figure 10, B**). Prior to the production of an ECM, SA produces a variation of factors that help prevent detachment of the newly produced daughter cells. An ECM is produced as a fraction of SA die, releasing extracellular DNA (eDNA) and cytoplasmic proteins into its surroundings[59].

For SA specifically, *exodus* occurs once the bacterial cells have proliferated followed by *maturation* (**figure 10, C and D**). *Exodus* is a process that takes place in the early stages of biofilm formation, where several cells from within the biofilm are released shortly after *multiplication*. The immature SA biofilm secretes a nuclease that initiates the nuclease-dependent degradation of eDNA, resulting in *exodus*. *Maturation* is the process in which three-dimensional microcolonies are formed by rapid division of the remaining bacterial cells post *exodus*. The microcolonies are composed of eDNA and proteins such as phenol soluble modulin (PSM)[59].

Dispersal occurs when cells and cell-clusters detach from the biofilm, and this step enables cells to spread to other infection sites through the blood and extracellular fluids (**figure 10, E**). It has been shown that *dispersal* in SA biofilms is controlled by accessory gene regulator (AGR) quorum sensing, which depends on multiple factors such as cell density and the accumulation of autoinducers[59].

Biofilms are notorious for their resistance towards modern antibiotics and causes many bacterial infections, some of which are chronical. SA produces biofilms in the lungs of cystic fibrosis patients which can lead to respiratory failure because of progressive lung damage. Furthermore, SA biofilms are the most frequent causes of infection in implant-associated infections such as artificial heart valves, coronary stents, and central venous catheters. As most infections caused by SA biofilms are either methicillin or multiply drug resistant, treatment is very limited[59,61]. It is estimated that 80 % of bacteria responsible for chronical diseases produce biofilms[62]. In comparison to a single bacterial cell, it requires 10 – 1000 times the concentration of an antibiotic agent to kill the same bacteria within a biofilm[61,67].

1.6 Solid-phase peptide synthesis

Solid-phase peptide synthesis (SPPS) is the preferred method to produce longer peptides, and it was developed in the early 1950's by the American biochemist Robert Bruce Merrifield. The novel method allowed chemists to chemically synthesise almost any peptide including hormones and toxins. In 1984, Merrifield received a Nobel Prize in Chemistry for his invention[68,69].

SPPS is a powerful tool within bioorganic chemistry, where the *C*-terminal of the first AA is attached to an insoluble solid support allowing the alpha-amine to react with an activated ester of another AA forming a peptide bond (**figure 11**). SPPS builds upon protecting group chemistry, where functional groups within a molecule are masked thus allowing selected groups to react. Protecting groups are applied to AAs with sidechains containing -NH_2, -OH, -SH, -COOH or other reactive functionalities[70–72].
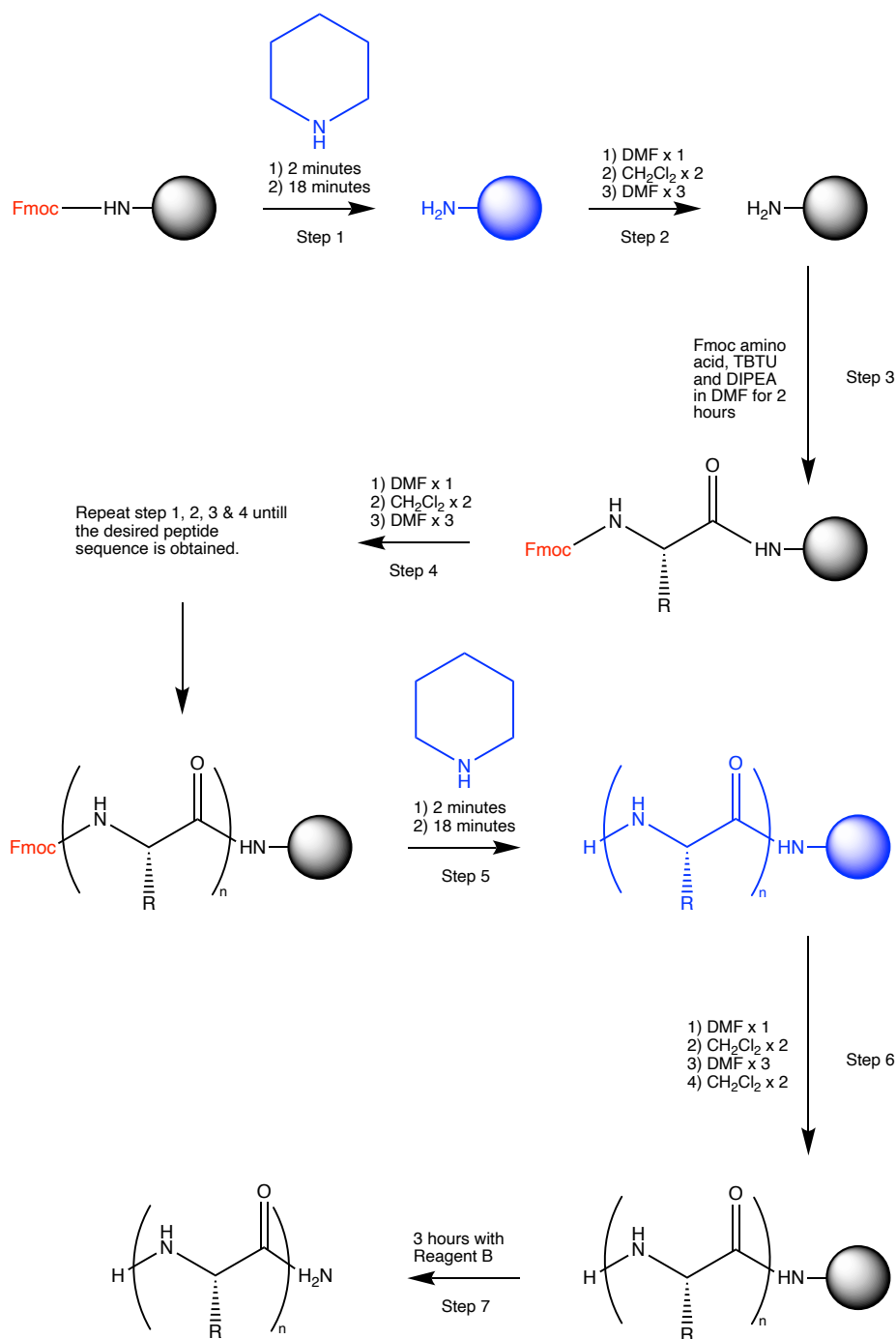
Figure 11: Overview of peptide synthesis (SPPS)[12]

The figure illustrates the peptide synthesis using Fmoc-chemistry on solid-phase. In step 1, the Fmoc protecting group on the amide rink resin is removed with piperidine ((CH₂)₅NH) followed by step 2, where excess piperidine is removed through a washing procedure using DMF and CH₂Cl₂. In step 3, an AA is coupled to the resin using the coupling reagent TBTU and base such as DIPEA in DMF and left to react for 2 hours. In step 4, excess reagents from step 3 are removed through a washing procedure using DMF and CH₂Cl₂. Step 1 through 4 are repeated until the desired peptide is obtained. Once the desired peptide is synthesised, the Fmoc protecting group on the last AA is removed with piperidine (step 5) followed by step 6, where excess piperidine is removed through a washing procedure using DMF and CH₂Cl₂. Step 6 includes an additional wash with CH₂Cl₂ to prepare the peptide decoupling. Finally, the peptide is cleaved from the amide rink resin using reagent B and left to react for 3 hours. The illustration was prepared with ChemDraw.

In SPPS, protecting groups are divided into permanent protecting groups and temporary protecting groups. Permanent protecting groups are removed at the end of the synthesis, and these include sidechain and *C*-terminal protecting groups such as tert-butoxycarbonyl (Boc), *tert*-butyl (*t*Bu) and triphenylmethyl (Trt). These protecting groups are acid-labile and are removed with trifluoroacetic acid (TFA) [70–72].

In contrast, temporary protecting groups are removed following each coupling step in the synthesis and include α-amino protecting group. The most common alpha-amino protecting group is fluorenyl methoxycarbonyl (Fmoc), which is a base-labile protecting group[72]. Fmoc is removed following each step in the synthesis with a solution of 20 % piperidine in *N,N*-dimethylformamide (DMF) (**figure 12**)[70–72].
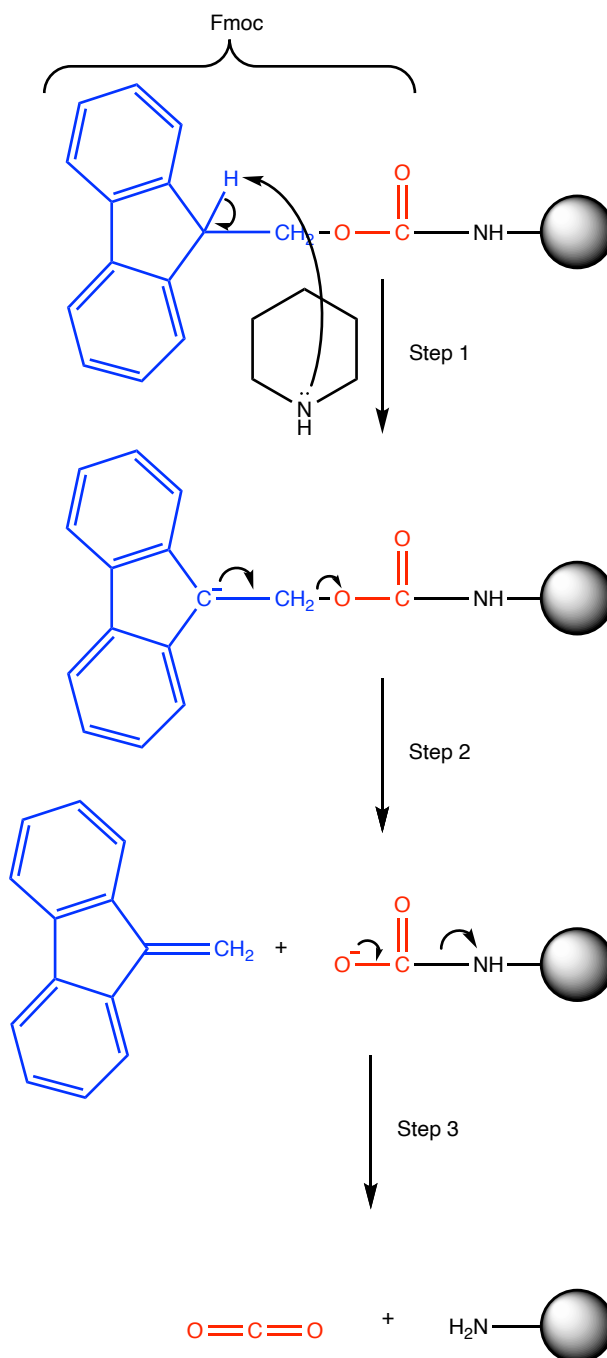
Figure 12: Fmoc deprotection mechanism[70]

The figure illustrates the mechanism behind Fmoc deprotection of an amino acid. The Fmoc-group collapses into dibenzofulvene (blue) and CO_2 (red) following treatment with piperidine. The illustration was prepared with ChemDraw.

AIMS AND OBJECTIVES

It has previously been shown that silver coordinates to cysteine residues and that this coordination induces alpha helicity between cysteines in positions $i,i+4$[12]. Previously, other metal-ions have been tested, but only Ag^+ induced alpha-helicity[11]. Furthermore, it has been established that there is a correlation between the overall charge of an AMP and an increased antimicrobial activity[3].

On that basis, the aim of this thesis was to investigate whether the antimicrobial activity of the derivatives based on the alpha-helical region within Tenecin 1 against SA will improve following the addition of silver. Firstly, we aimed to synthesise four derivatives corresponding to the alpha-helical region of Tenecin 1, that consists of 11 AAs, two of which are cysteines in positions $i,i+4$. The four derivatives containing either single or double AA substitution. To investigate the importance of cysteine residues within the fragments, four additional derivatives containing serine instead of cysteine were synthesised. Based on the results obtained by Ahn and co-workers[11], peptide **4** exhibited the greatest potential regarding antimicrobial activity in comparison to peptide **1 – 3**. On that note, fragments with different overall charges were synthesised based on peptide **4** to investigate the relationship between charge and antimicrobial activity.

To ensure that the correct peptides were obtained following their synthesis, retention times and molecular weights (MWs) were recorded for each peptide using analytical methods such as high-performance liquid chromatography (HPLC) and liquid chromatography–mass spectrometry (LC-MS). Once confirmed, the peptides were purified using the preparatory HPLC and the fractions of interest were collected. Following this, Ag^+ was added to analyse and quantify whether its coordination to the peptide had a stabilising effect on the alpha-helical structure. To investigate whether Ag^+-coordination had an impact on the secondary structure of the peptides, methods such as CD were used to analyse peptides with and without Ag^+ addition. To investigate whether Ag^+ remains coordinated to the peptide over time, a CD-spectrum was recorded on day 0 and day 5.

To investigate the antimicrobial activity of the peptides with and without the addition of Ag^+ against SA, MIC-values were measured and compared against each other. Based upon the MIC-values, the peptide(s) with Ag^+-addition exhibiting the highest antimicrobial activity (i.e., the lowest MIC-value) were selected to perform a biofilm-assay against SA. Finally, the same peptides were selected to perform a haemolysis assay on human red blood cells (RBCs).

2. METHODS AND MATERIALS

2.1 Peptide design and synthesis

To synthesise the peptides corresponding to the alpha-helical region of Tenecin 1, a classical SPPS method was used (**section 5.1.1 – 5.1.4**). The method can be automated, but we performed it manually. 0.4g of resin was used for each peptide synthesis and all AAs used were Fmoc-protected. The synthesised peptides can be seen in the table (**table 1**) (**appendices figure 1 – 5**).

Table 1: Overview of synthesised peptides

The table gives an overview of the synthesised peptides including their peptide names, amino acid sequences and molecular weights.

Peptide name	Amino acid sequences	Molecular weight
1	DAACAAHCLWR	1215.4 g/mol
2	KAACAAHCLWR	1228.5 g/mol
3	DAACAAKCLWR	1206.4 g/mol
4	KAACAAKCLWR	1219.5 g/mol

Likewise, the modified peptides (containing serine instead of cysteine units) as well as the peptides with extra charge were synthesised manually by using SPPS (**section 5.1.5 – 5.1.13**), and these peptides can be seen in the table (**table 2**) (**appendices figure 1, 6 – 12**).

Table 2: Overview of synthesised peptides with modifications

The table gives an overview of the peptides that have been modified including their names, amino acid sequences, and molecular weights.

Peptide name	Amino acid sequence	Molecular weight
S1	DAASAAHSLWR	1183.4 g/mol
S2	KAASAAHSLWR	1196.5 g/mol
S3	DAASAAKSLWR	1174.4 g/mol
S4	KAASAAKSLWR	1187.5 g/mol
4c$^+$	KAACAAKCLWRR	1375.6 g/mol
4n$^+$	RKAACAAKCLWR	1375.6 g/mol
4c$^+$n$^+$	RKAACAAKCLWRR	1531.7 g/mol

Lastly, two other peptides, **AC** and **ENDO** (endomorphin 1) were synthesised, where **AC** was used as a test peptide and **ENDO** were used as a negative control (**table 2**) (**appendices figure 1, 13 and 14**).

Table 3: Overview of synthesised peptides used as controls

*The table gives an overview of the peptide **ENDO** (negative control) and **AC** (test peptide) including their names, amino acid sequences, and molecular weights.*

Peptide name	Amino acid sequence	Molecular weight
ENDO	YPWF	611.4 g/mol
AC	Ac-RCAAAC	634 g/mol

2.2 Purity investigation and validation

Analytical HPLC was performed for all peptide samples prior to their purification. This was done by mixing a small amount ($\sim 20 \mu L$) of the concentrated samples from the water phase with 30 % acetonitrile (MeCN) ($300 \mu L$) (**section 5 and 5.1**). After approval on the analytical HPLC, the evaporated water phase was mixed with 20 % MeCN (5 – 10 mL) and was run on the preparatory HPLC either as a single or as two injected fractions. The elution fractions with distinct peaks were repeatedly tested on the analytical HPLC, where a drop was mixed with 30 % MeCN (1 mL). The now approved fractions were collected and freeze-dried (**section 5 and 5.1**). After freeze drying, the peptide (1 mg) and 20 % MeCN ($300 \mu L$) were mixed and analysed by LC-MS (**section 5**).

2.3 Peptide concentration determination

To determine the concentration of the individual peptides with ultraviolet–visible spectroscopy (UV-vis), two different methods were used. The first method utilised a 4,4'-dithiodipyridine (DTDP) UV-vis method and was used for peptides containing cysteine units. The peptide concentration was determined based on measuring the content of free thiols within the peptides[73].

Stock solutions (containing 1 mg peptide in 1 mL MilliQ water) were prepared for all peptides. A specific volume of stock solution was mixed with phosphate buffer (pH 7.2, 10 mM) to obtain a final thiol concentration of <40 μM and a final volume of 1 mL (**table 4**).

To this mixture, EDTA buffer (200 μL, pH 6.8, 0.2 mM) and DTDP (50 μL, 4 mM) were added, then vortexed and incubated for 5 minutes. From each stock solution, three samples were prepared.

Furthermore, two blank samples were prepared, one of which contained DTDP without peptide and the other contained peptide without DTDP. Finally, each sample was run on the UV-vis, and the absorbance at 324 nanometres (nm) was recorded (**section 5**).

Peptide name	Volume peptide stock solution (mL)	Volume phosphate buffer (mL)
1	0.024	0.976
2	0.025	0.975
3	0.024	0.976
4	0.024	0.976
AC	0.013	0.987
$4n^+$	0.028	0.972
$4c^+$	0.028	0.972
$4c^+n^+$	0.031	0.969

Another method was used for the peptides without cysteine units. This method involved measuring the absorbance of tryptophan within each sample[74]. For each peptide, three samples were prepared with a dilution factor of 1:32, 1:34, 1:36, respectively, which contained peptide stock solution (containing 1 mg peptide in 1 mL MilliQ water) with phosphate buffer (pH 7.2, 10 mM). Lastly, the absorbance at 280 nm (signal for tryptophan) was recorded and noted (**section 5**).

2.4 Structure investigation with and without silver

CD was used to investigate the structure of each peptide with and without the addition of silver. Based on literature, the amount of silver must be equivalent to 2 to achieve the highest alpha-helicity[12]. Based on the peptide concentrations that were determined by UV-vis, the amount of silver corresponding to 2 equiv. could be found.

2.4.1   HPLC titration

In addition to this, we performed a titration experiment on the analytical HPLC where various equivalents of silver were added to peptides **AC** and **4**. Samples were prepared by mixing a peptide stock solution (containing 1 mg peptide in 1 mL MilliQ water, 100 *L*) with phosphate buffer (pH 7.2,

10 mM, 375 μL), and adding different amounts of silver solution, which corresponded to a silver concentration of 0.5 equiv., 1 equiv., 1.5 equiv., 2 equiv. and 2.5 equiv. Afterwards, all samples were run on the analytical HPLC and data was collected (**section 5**).

2.4.2 Circular dichroism

Samples without the addition of silver were prepared by mixing peptide stock solution (containing 1 mg peptide in 1 mL MilliQ water, 100 μL), with MilliQ water (25 μL) and phosphate buffer (pH 7.2, 10 mM, 375 μL). This was done for all peptides except for peptide **ENDO** due to its length.

Samples containing silver were prepared by mixing peptide stock solution (containing 1 mg peptide in 1 mL MilliQ water, 100 μL), phosphate buffer (pH 7.2, 10 mM, 375 μL) and a specific amount of silver solution (in MilliQ water, 25 μL) corresponding to 2 equiv. This was done for all peptides except for peptide **ENDO**. Additionally, a blank sample was prepared consisting of phosphate buffer (pH 7.2, 10 mM, 375 μL) and MilliQ water (125 μL). All samples were run on the CD instrument in triplicates (**section 5**). For selected samples (peptide **AC** and **4c$^+$**), CD samples were run over an extended period (day 0 and day 5).

2.4.3 NMR

^{1}H-NMR spectra were recorded for all peptides. Furthermore, ^{19}F spectra for selected peptides (peptide **AC** and **ENDO**). Samples for ^{1}H-NMR were prepared by mixing $\sim 5 mg$ peptide with either 600 μL water/D_2O, DMSO-d_6 or D_2O. TMS was added to D_2O as an internal reference (**table 5**). ^{1}H-NMR spectra were measured for each sample.

Table 5: Overview of solvent used in ^{1}H-NMR samples.

The table shows the different peptides and the solvent used for preparation of their 1H-NMR samples.

Peptide name	Solvent
1, 2, 3, 4, S1, S2, S3, S4, 4c$^+$, 4n$^+$, 4c$^+$n$^+$	90 % H_2O + 10 % D_2O (600 μL)
ENDO	DMSO-d_6 (600 μL)
AC	D_2O (600 μL)

For peptide **AC** and **ENDO**, samples for ^{19}F were prepared by mixing 2,2,2-trifluoroethanol (TFE) (1 μL) to the already-prepared ^{1}H-NMR-samples. Following the addition of TFE, ^{19}F spectra and a new ^{1}H-NMR spectra were recorded (**section 5 and appendices figure 57 – 73**).

2.5 Biological assays

Results obtained by Ahn and co-workers[11] showed that the peptides exhibited the greatest potential as antimicrobial agents against *SA*, i.e., the lowest MIC values, and on that basis, all biological experiments were performed using *SA*.

Prior to the experiments, stock solutions with a starting concentration of 533 $\mu g/mL$ were prepared for all peptides (peptides **1 – 4**, peptides **S1 – S4**, **AC**, **ENDO**, **4c$^+$**, **4n$^+$** and **4c$^+$n$^+$**), Melittin and Polymyxin B. Likewise, stock solutions for all our peptides (peptides **1 – 4**, peptides **S1 – S4**, **AC**, **4c$^+$**, **4n$^+$** and **4c$^+$n$^+$**) with 2 equiv. of Ag$^+$ added were prepared (**table 6**). Furthermore, a stock solution with a starting concentration of 763 $\mu g/mL$ was prepared of Ag$^+$. This concentration was chosen based on the highest mass of Ag$^+$ (being 0.0023 g) added to the peptide stock solution. Between experiments, all stock solutions were stored at -20 °C[75].

Moreover, lysogeny broth (LB)-agar plates and Mueller-Hinton broth (MHB)-media were prepared and used for MIC assays, and TSB-media was prepared for biofilm assays.

Table 6: Overview of the amount of Ag⁺ added to the peptide samples.

The table gives an overview of the amount of Ag⁺ added to the different peptide samples. The 2ⁿᵈ column of the table shows the different number of moles of each peptide based upon the results obtained from the UV-vis experiments. The number of moles of Ag⁺ corresponding to 2 equiv. of peptide is shown in the 3ʳᵈ column, and the 4ᵗʰ column shows the mass of Ag⁺ added to each solution to obtain 2 equiv. of Ag⁺. Furthermore, the table shows the concentration of silver in the different stock solution (5ᵗʰ column) and the final concentration of Ag⁺ in the first well in the MIC experiment.

Peptide name	$n_{peptide}$ [mol]	n_{Ag+} corresponding to 2 equiv. [mol]	m_{Ag+} added [g]	Concentration of Ag⁺ in the stock solution [µg/mL]	Concentration of Ag⁺ in the 1ˢᵗ well [µg/mL]
1 w. Ag⁺	4,79E-06	9.57E-06	0.0016	533	133.25
2 w. Ag⁺	2,95E-06	5.90E-06	0.0010	333	83.25
3 w. Ag⁺	6,74E-06	1.35E-05	0.0023	763	190
4 w. Ag⁺	3,83E-06	7.66E-06	0.0013	433	108.25
S1 w. Ag⁺	1,86E-06	3.72E-06	0.0006	210	52.5
S2 w. Ag⁺	1,88E-06	3.76E-06	0.0006	210	52.5
S3 w. Ag⁺	1,96E-06	3.92E-06	0.0006	220	55
S4 w. Ag⁺	2,12E-06	4.23E-06	0.0007	230	57.5
4n⁺ w. Ag⁺	5,30E-06	1.06E-05	0.0018	600	150
4c⁺ w. Ag⁺	2,59E-06	5.18E-06	0.0009	290	70.5
4c⁺n⁺ w. Ag⁺	2,58E-06	5.15E-06	0.0009	290	70.5
AC w. Ag⁺	2,40E-06	4.81E-06	0.0008	270	67.5

2.5.1 Minimum inhibitory concentration

On day 1, *SA* (subspecies *aureus* strain Wichita[76]) were cultivated on a Petri dish. On day 2, bacteria from the Petri dish were inoculated and transferred into a tube containing 4 mL MHB-medium. The tubes were incubated overnight (ON) at 37 °C with shaking (150 rounds per minutes (rpm)). This was done twice to obtain two different ON cultures[77–79].

On day 3, 100 μL of each stock solution was mixed with 100 μL MHB-medium. The 200 μL of each test substance was transferred to the top row of the 96-well MIC-plate (1A – 10A) giving a concentration of 266.5 $\mu g/mL$ for each test substance except Ag⁺. 100 μL of MHB-medium was added to columns 1 – 10 rows B – H, and 100 μL of test substance was transferred from row A to row B. This step was repeated between each row (rows C – H), giving a twofold dilution for each row. Lastly, 100 μL test substance was removed from wells 1H – 10H[77–79].

The ON cultures, which were prepared on day 2, were diluted to obtain an absorbance of 0.1 at OD_{600}. Just before use, OD_{600} was adjusted to an absorbance of 0.01 through dilution with MBH-medium. 100 μL of diluted ON culture was added to columns 1 – 10 rows A – H. Wells 11 A – 11 H were used as a negative control and contained 100 μL MHB-medium and 100 μL bacteria. Similarly, wells 12 A – 12 H were used as a positive control and contained 200 μL MBH-medium[77–79].

The final concentration of each test substance in wells 1 A – 10 A (except for Ag^+) post addition of 100 μL ON culture was 133 $\mu g/mL$. The lowest concentration of test substance tested for was 1.04 $\mu g/mL$ in wells 1 H – 10 H. Once all wells were filled, the MIC-plates were placed in plastic bags and incubated at 37 °C for 16 – 18 hours[77–79].

The assay was performed twice in duplicates for peptides **1 – 4**, peptides **S1 – S4**, **4c⁺**, **4n⁺** and **4c⁺n⁺**, where two different ON cultures were used.

On day 4, the MIC-values were determined based upon the lowest concentration of test substance showing no visible bacterial growth[77–79].

In parallel, an in-depth MIC-assay was preformed to determine the MIC-value of Ag^+. The setup remains the same, but a concentration of Ag^+ as low as 0.093 $\mu g/mL$ was investigated.

2.5.1.1 Spot test

Based upon the results obtained from the MIC-assay, selected concentrations for the various peptides (**figure 7**) were selected. To investigate whether the specific concentration of test substance was bactericidal or bacteriostatic, the MIC-value and the concentration above were spotted on LB-agar plates. The plates were placed in plastic bags and incubated at 37 °C for 16 – 18 hours.

Table 7: Overview of the peptides and their concentration selected for spot test

The table shows the peptides and their concentrations that were selected for spot test. The 1ˢᵗ concentration is equalled to the MIC-value, and the 2ⁿᵈ concentration is 2-fold higher than the concentration of the MIC-value.

Peptide name	1ˢᵗ concentration	2ⁿᵈ concentration
1 w. Ag^+	$2.08\ \mu g/mL$	$4.15\ \mu g/mL$
2 w. Ag^+	$8.31\ \mu g/mL$	$16.63\ \mu g/mL$
3 w. Ag^+	$4.15\ \mu g/mL$	$8.31\ \mu g/mL$
4 w. Ag^+	$8.31\ \mu g/mL$	$16.63\ \mu g/mL$
S1 w. Ag^+	$2.08\ \mu g/mL$	$4.15\ \mu g/mL$
S2 w. Ag^+	$2.08\ \mu g/mL$	$4.15\ \mu g/mL$
S3 w. Ag^+	$2.08\ \mu g/mL$	$4.15\ \mu g/mL$
S4 w. Ag^+	$2.08\ \mu g/mL$	$4.15\ \mu g/mL$
4n⁺	$133\ \mu g/mL$	$133\ \mu g/mL$
4n⁺ w. Ag^+	$2.08\ \mu g/mL$	$4.15\ \mu g/mL$
4c⁺ w. Ag^+	$2.08\ \mu g/mL$	$4.15\ \mu g/mL$
4c⁺n⁺ w. Ag^+	$4.15\ \mu g/mL$	$8.31\ \mu g/mL$
AC w. Ag^+	$33.25\ \mu g/mL$	$66.5\ \mu g/mL$
Pure Ag^+	$0.745\ \mu g/mL$	$1.49\ \mu g/mL$

2.5.2 Biofilm

Based on the results obtained from the MIC assay, samples were prepared from the stock solution and used for the biofilm assay. The samples had a varying concentration corresponding to 1.04 – 16.63 $\mu g/mL$ once added to the wells. A summary of the selected peptides and their concentrations can be seen in **table 8**.

Table 8: **Overview of the peptides and their concentration selected for biofilm assay**

The table gives an overview of the peptides and concentrations selected for the biofilm assay, which was based upon the results obtained in the MIC-assay. The 1st concentration corresponds to a concentration that is 2-fold lower than the MIC-value, the 2nd concentration corresponds to the MIC-value and the 3rd concentration corresponds to a concentration that is 2-fold higher than the MIC-value. The individual MIC-values for each peptide were determined during the MIC-assay.

Test substance	1st concentration [$\mu g/mL$]	2nd concentration [$\mu g/mL$]	3rd concentration [$\mu g/mL$]
1 w. Ag$^+$	1.04	2.08	4.15
2 w. Ag$^+$	4.15	8.31	16.63
3 w. Ag$^+$	2.08	4.15	8.31
4 w. Ag$^+$	4.15	8.31	16.63
4c$^+$ w. Ag$^+$	1.04	2.08	4.15
4n$^+$ w. Ag$^+$	1.04	2.08	4.15
4c$^+$n$^+$ w. Ag$^+$	2.08	4.15	8.31
Ag$^+$	0.372	0.745	1.49

On day 1, *SA* (subspecies *aureus* strain Wichita) were cultivated on a Petri dish. On day 2, bacteria from the Petri dish were inoculated and transferred into a tube containing 4 mL TSB-medium. The tubes were incubated ON at 37 °C with shaking (150 rpm). This was done twice to obtain two different ON cultures[80].

On day 3, the ON cultures were diluted 100-fold in TSB-medium 2 % (w/v) glucose. 190 μL of diluted ON culture was transferred to the wells of a flat bottom 96-well plate. Each sample and test-condition were tested in triplicates. Furthermore, two controls were run in parallel; the first control contained 200 μL TSB-medium and the second control contained 200 μL diluted ON culture. The 96-well plates were placed in plastic bags and incubated at 37 °C for 24 hours. Each plate was duplicated.

On day 4, 10 μL of the selected test substances (**table 8**) were added to each well. The plates were placed in plastic bags and incubated at 37 °C for 24 hours[80].

On day 5, the media was carefully removed from each well without disturbing the biofilm. Subsequently, each well was washed three times with sterile saline (200 µL, 0.9 %) to remove planktonic bacterial cells, and the plates were left to air-dry. Following this, ethanol (200 µL, 96 %) was added to each well to fix the biofilm. Excess ethanol was removed, and the plates were left to air-dry. Crystal Violet (CV) (200 µL, 0.1 %) was added to each well, and left to incubate at room temperature for 10 minutes. Afterwards, CV was removed, and the wells were washed three times with MilliQ-water (200 µL). Once again, the plates were left to air-dry. Following this, ethanol (200 µL, 96 %) was added to each well and mixed well. The content from each well was transferred to a clean flat bottom 96-well plate, and CV at OD_{595} was measured using a plate-reader[80]. If the measurements for the absorbance were over 0.8, the content of the wells were diluted 2 to 10-fold.

2.5.3 Haemolysis assay

Firstly, 10 samples consisting of 10 mL of human blood was drawn into plasma tubes coated with EDTA (an anti-coagulant). To purify the human RBC, each sample was centrifuged at 800×g for 15 minutes, and afterwards the plasma fraction was removed. The pellet was washed with NaCl (10 mL, 0.9%) and centrifuged. The supernatant was removed. This procedure was repeated 5 times[81,82].

Peptides and their concentrations were selected based on the results obtained from the MIC assay (**table 8**). The concentrations correspond to the peptides' MIC-values as well as a concentration above- and below. The peptides were diluted in NaCl (0.9%). 100 µL of each solution was added to a 96-well MIC-plate. A solution of Triton X-100 (100 µL, 1%) in NaCl (0.9%) was prepared and used as a positive control, and NaCl (0.9 %) was used for baseline correction. The experiment was performed twice[81,82].

Afterwards, 100 µL RBCs was added to the 96-well MIC-plate to reach a final volume of 200 µL, and lastly, the plates were incubated at 37 °C for 20 hours[81,82].

The following day 20 µL of supernatant was transferred to the wells of a flat bottom 96-well plate, and NaCl (100 µL, 0.9 %) was added. The OD_{546} was measured using a plate-reader, and the percentage of haemolysis induced by the peptides was calculated[81,82].

3. RESULTS AND ANALYSIS

3.1 Purity investigation and validation

3.1.1 Analytical HPLC

All spectra for each of the peptides **1 – 4** exhibit one clear and prominent signal at a retention time between 4.6 and 4.7 minutes. All peptides exhibit a signal at 1.8 minutes, although the peak vary in intensity. This peak could be TFA. Furthermore, the spectrum for peptide **3** exhibits a "shoulder", and the spectrum for peptide **4** exhibits a smaller peak at a retention time of 4 minutes, this peak could be an impurity. Besides that, no other peaks are recorded (**appendices figure 15 – 18**).

Likewise, one clear and prominent signal is recorded at a retention time between 4.5 – 4.6 minutes on each spectrum for peptides **S1**, **S3** and **S4**, which is assumed to be the desired peptides. On the spectra for sequence **S2**, the signal at 4.5 minutes is split into two peaks, which could be a sign of impurity or a diastereomer. Furthermore, all peptides exhibit a signal at 1.8 minutes, which is assumed to be TFA (**appendices figure 19 – 22**).

For sequences **4c$^+$**, **4n$^+$**, **4c$^+$n$^+$**, one clear and prominent signal is recorded on each spectrum at a retention time between 4.5 – 4.6 minutes. The signal at 1.8 is also visible in these spectra. In the spectrum for peptides **ENDO** and **AC**, one clear and prominent signal is recorded at 5.3 minutes and 4.1 minutes, respectively. The spectrum for **AC** shows a disturbed waterline (**appendices figure 23 – 27**).

3.1.2 LC-MS

The LC-MS-spectra for peptides **1 – 4** all show a higher m/z than expected. For peptide **1**, a m/z of 1284.55 g/mol was recorded, which is 69.1 m/z higher than the expected weight of 1215.4 g/mol for a M$^+$-ion. The additional 69.1 m/z could originate from three additional Na$^+$-ions (molecular weight (MW): 22.98 g/mol). For peptide **2**, a m/z of 1286.57 was recorded, which is 58 m/z higher than the expected M$^+$-weight of 1228.5 g/mol. This could suggest that a COOCH$_3^+$ (MW: 59 g/mol) has been bound to the peptide. The recorded m/z for peptides **3** and **4** were 1277.61 and 1290.68, respectively. The expected molecular weight for peptide **3** was 1206.4 g/mol, and 1219.5 g/mol for peptide **4**. Both peptides deviated from the expected m/z with 71.2 g/mol, which could suggest that CH$_3$OH + K$^+$ (MW: 71 g/mol) have been bound to the peptides (**appendices figure 30 – 33**).

The LC-MS-spectra of peptides **S1** through **S4** all show a signal corresponding to the expected m/z, which suggests that it is the M[+]-ion that can be seen (**S1**: 1183.58 g/mol; **S2**: 1196.65 g/mol, **S3**: 1174.62 g/mol; **S4**: 1187.69 g/mol) (**appendices figure 34 – 37**).

The LC-MS-spectra for peptide **4c[+]** (MW: 1375.6 g/mol) exhibited a signal at 688.3780 m/z, which corresponds to the (M+2)/2-ion. On a similar note, peptide **4c[+]n[+]** (MW: 1531.7 g/mol) exhibited a signal at 766.42 m/z, which also corresponds to the (M+2)/2-ion. Peptide **4n[+]** (MW: 1375.6 g/mol) exhibited a signal at 687.37 m/z, which corresponds to half of the expected mass, and therefore, the signal could show the M/2-ion (**appendices figure 38 – 40**).

The LC-MS-spectra for **ENDO** exhibited a signal at 611.29 m/z, which corresponds to the M[+]-ion, whereas **AC** showed a signal at 635 m/z, which corresponds to the M+1-ion (**appendices figure 41 and 42**).

3.2 Determination of peptide concentration

3.2.1   Calculation based on DTDP method

To determine the actual concentration of the peptides that contain cysteine units, the content of free thiols (molSH) within the peptide was measured using DTDP. The absorbance of pyridine-4(1H)-thione is measured. Pyridine-4(1H)-thione is present once DTDP is reduced by the free thiols, and on that basis, it is possible to calculate molSH using **equation 1**[12,73]:

$$molSH = 0.00125L * (A_{324_1} - A_{324_2} - A_{324_3})/(\Delta\varepsilon_{324} * 1cm)$$

Equation 1[73]

0.00125 L is the total volume of the sample, 1 cm refers to the length of the cuvette and $\Delta\varepsilon_{324}$ is a standard value which corresponding to $21400\ M^{-1}cm^{-1}$ in this case[73].

Firstly, we know that the ratio between the number of thiols and peptides is 2:1, as there are two cysteine residues in each peptide. Moreover, we know the exact volume (v) of peptide stock solution within each sample. On that basis it is possible to calculate the concentration of pure peptide (**table 9**).

Table 9: Overview of the peptide concentration and calculations

The table shows the mean absorbance of pyridine-4(1H)-thione, the number of moles of thiols calculated based on equation 1, the number of moles of peptide and lastly, the actual concentration of each peptide.

Peptide name	Mean absorbance w/o blank	Thiol [mol]	Peptide [mol]	$C_{peptide}$ [mol/L]
1	0.186	1.086E-08	5.432E-09	0.0002263
2	0.308	1.797E-08	8.986E-09	0.0003594
3	0.134	7.827E-09	3.914E-09	0.0001630
4	0.462	2.697E-08	1.348E-08	0.0002809
AC	0.735	4.293E-08	2.147E-08	0.0016512
$4n^+$	0.153	8.937E-09	4.468E-09	0.0001595
$4c^+$	0.313	1.828E-08	9.141E-09	0.0003264
$4c^+n^+$	0.281	1.641E-08	8.207E-09	0.0002647

3.2.2 Calculation based on the Trp method

For the samples that did not contain cysteine, we used a second method to determine the concentration of peptide within the samples. We measured absorbance of tryptophan, and used **equation 2** to calculate the concentration of peptide:

$$mg\ peptide\ per\ ml = (A_{280} * DF * MW)/e$$

Equation 2[74]

e is the molar extinction coefficient and is equalled to 5560 for tryptophan. Besides tryptophan, **_ENDO_** also has tyrosine (*e = 1200*), and therefore the two extinction coefficients are summed up to calculate its concentration[74]. Three measurements with different dilution factors (DF) were performed for each peptide (**table 10 and 11**).

Table 10: Measurements of OD$_{280}$ for peptides w/o cysteine using the Trp method

The table shows three different measurements at three different dilution factors for each peptide with the blank sample subtracted.

Peptide name	1.Measurement w/o blank (DF=1:32)	2.Measurement w/o blank (DF=1:34)	3.Measurement w/o blank (DF=1:36)
S1	0.051	0.048	0.057
S2	0.047	0.050	0.054
S3	0.047	0.052	0.051
S4	0.042	0.049	0.045
ENDO	0.114	0.127	0.131

Table 11: Calculation of concentration of each peptide w/o cysteine

The table shows mg peptide/mL (which was calculated based on equation 2) at different dilution factors and the mean mg peptide/mL.

Peptide name	mg peptide/mL (DF=1:32)	mg peptide/mL (DF=1:34)	mg peptide/mL (DF=1:36)	Mean mg peptide/mL
S1	0.757	0.671	0.753	0.727
S2	0.705	0.707	0.722	0.711
S3	0.692	0.722	0.669	0.694
S4	0.626	0.688	0.597	0.637
ENDO	0.719	0.755	0.736	0.737

Finally, the concentration of peptide (mol/L) was calculated using the molar mass of each peptide (**tables 11 and 12**).

Table 12: Concentration of each peptide w/o cysteine based on the Trp method.

The table shows the final concentration for each peptide without cysteine in mol/L.

Peptide name	Concentration of peptide [mol/L]
S1	0.0066
S2	0.0006
S3	0.0006
S4	0.0005
ENDO	0.0012

3.3 Structure investigation

3.3.1 HPLC-titration experiment

The HPLC-titration experiment was carried out for **AC** (**figure 13**) and peptide **4** (**appendices figure 28**). For **AC**, an intense peak was measured at 4.1 minutes with the addition of 0.5 equiv. of silver (**figure 13, A**). The intensity of the peak at 4.1 minutes decreased, and a new broad peak between 4.4 – 4.8 minutes emerged following the addition of silver at higher equivalents. Decrease of the peak at 4.1 minutes indicates a decrease in unbound peptide, whereas the increase in a new broad peak at 4.4 – 4.8 minutes indicates an increase in silver-bound peptide.

The retention time increase following the addition of silver indicates that there is a connection between the retention time and the level of alpha-helicity[83,84], and therefore these results could further indicate that the level of alpha-helicity within **AC** increases as the equivalents of Ag^+ increases up to 2 equiv.

The HPCL-titration experiment for peptide **4** (**appendices figure 28**) showed no change except for a minor decrease in intensity at 4.6 minutes with 2.5 equiv. silver.

Figure 13: Analytical HPLC spectra for AC obtained from the HPLC-titration experiment

*The figure shows the results obtained from the HPLC-experiment for peptide **AC**. Spectrum **A** contained 0.5 equiv. Ag⁺, spectrum **B** contained 1 equiv. Ag⁺, spectrum **C** contained 1.5 equiv. Ag⁺, spectrum **D** contained 2 equiv. Ag⁺ and spectrum **E** contained 2.5 equiv. Ag⁺. All spectra were recorded at 215 nm.*
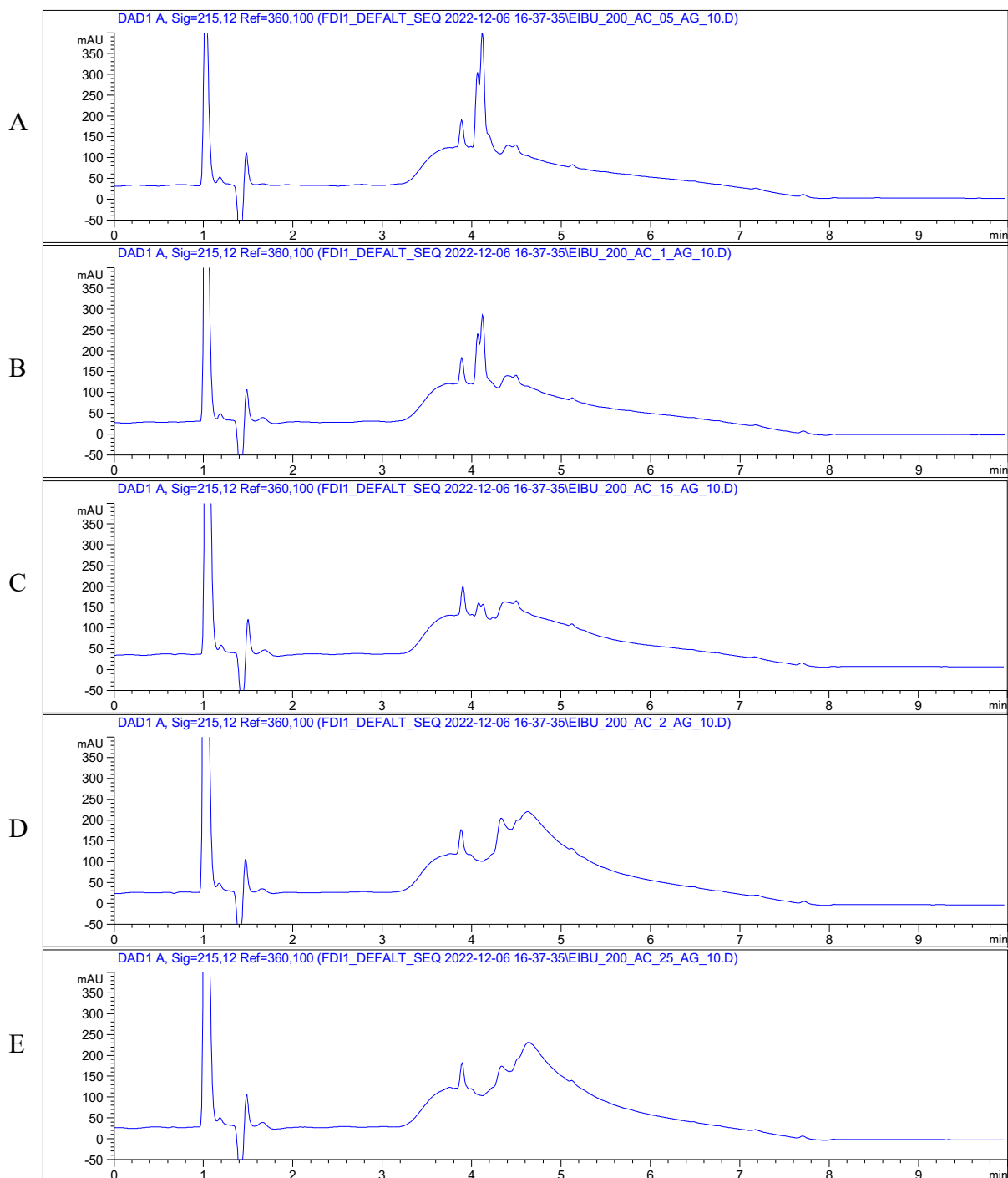
3.3.2   Circular dichroism data

A small change can be seen on the CD spectra for peptides **1 – 4** (**appendices figure 43 – 46**) following the addition of 2 equiv. of silver. Due to this minor change, the peptides exhibit a tendency towards an alpha-helical behaviour. This does not correspond to the results that we expected.

No significant change can be seen on the CD spectra for peptides **S1 – S4** (**appendices figure 47 – 50**) following the addition of silver, which we expected.
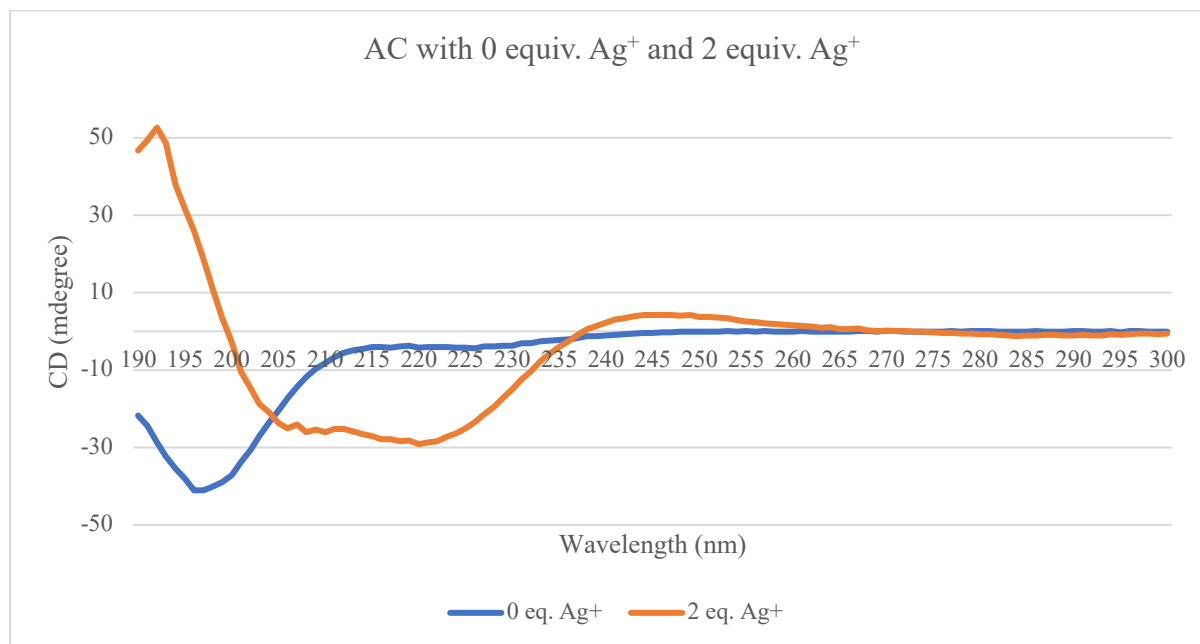
Graph 1: CD spectra for peptide AC with 0 equiv. Ag⁺ and 2 equiv. Ag⁺

*The graph shows the CD spectra recorded for peptide **AC** following the addition of 0 equiv. Ag⁺ and 2 equiv. Ag⁺. The blue curve indicates the measurements performed after the addition of 0 equiv. Ag⁺, and the orange curve indicates the measurements performed after the addition of 2 equiv. Ag⁺. The x-axis shows the wavelength in nm and the y-axis show the CD in mdegree.*

The CD spectra for peptide **AC** (**graph 1**) showed a significant change following the addition of 2 equiv. of silver. The graph illustrating **AC** without silver addition shows a negative band at 195 nm and 210 nm, which describes a peptide with a random coil secondary structure. While the graph following addition of silver shows negative bands at 208 nm and 222 nm and a positive band at 193 nm indicating an alpha-helical secondary structure[85].
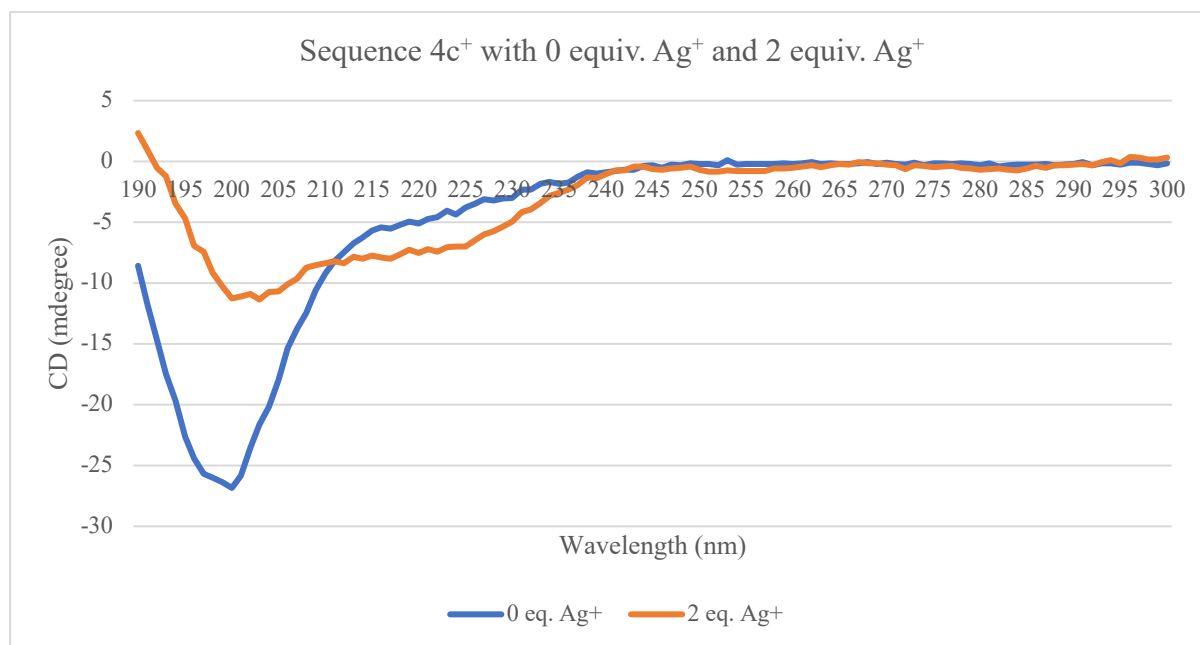
Graph 2: CD spectra for 4c⁺ with 0 and 2 equiv. Ag⁺.

*The graph shows the CD spectra recorded for peptide **4c⁺** following the addition of 0 equiv. Ag⁺ and 2 equiv. Ag⁺. The blue curve indicates the measurements performed after the addition of 0 equiv. Ag⁺, and the orange curve indicates the measurements performed after the addition of 2 equiv. Ag⁺. The x-axis shows the wavelength in nm and the y-axis show the CD in mdegree.*

Similarly, the CD spectra for peptide **4c⁺** (**graph 2**) showed a significant change following the addition of 2 equiv. of silver. The graph illustrating **4c⁺** without silver addition shows a negative band at 195 nm and 210 nm, which describes a peptide with a disordered secondary structure. While the graph following addition of silver shows negative bands at 208 nm and 222 nm and a slightly negative band at 193 nm. Overall, the graph indicates a tendency towards an alpha-helical secondary structure[85].
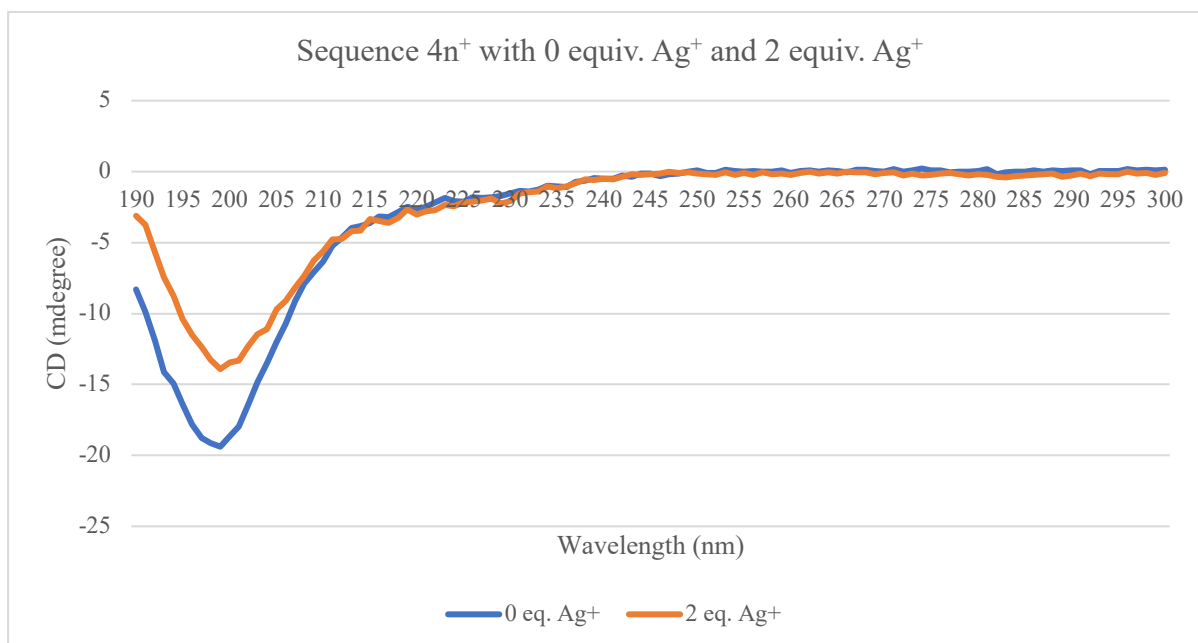
Graph 3: CD spectra for 4n⁺ with 0 and 2 equiv. Ag⁺.

*The graph shows the CD spectra recorded for peptide **4n⁺** following the addition of 0 equiv. Ag⁺ and 2 equiv. Ag⁺. The blue curve indicates the measurements performed after the addition of 0 equiv. Ag⁺, and the orange curve indicates the measurements performed after the addition of 2 equiv. Ag⁺. The x-axis shows the wavelength in nm and the y-axis show the CD in mdegree.*

Graph 4: CD spectra for 4c⁺n⁺ with 0 and 2 equiv. Ag⁺.

*The graph shows the CD spectra recorded for peptide **4c⁺n⁺** following the addition of 0 equiv. Ag⁺ and 2 equiv. Ag⁺. The blue curve indicates the measurements performed after the addition of 0 equiv. Ag⁺, and the orange curve indicates the measurements performed after the addition of 2 equiv. Ag⁺. The x-axis shows the wavelength in nm and the y-axis show the CD in mdegree.*

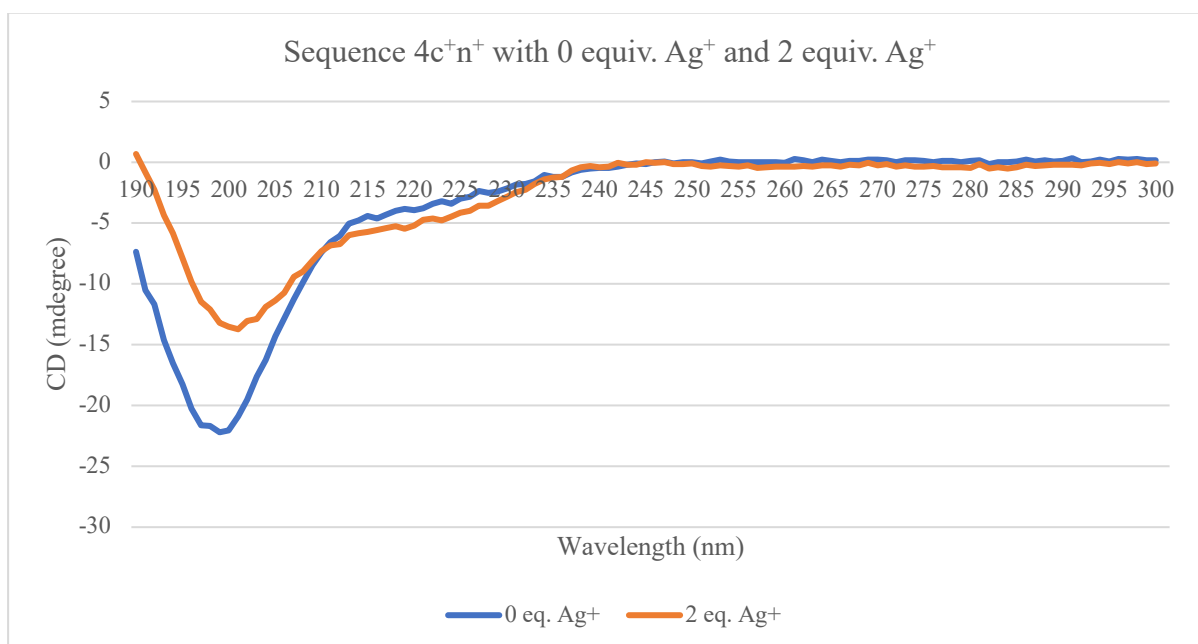Overall, both **4n⁺** and **4c⁺n⁺** (**graph 3 and 4**) show a minor change in secondary structure post addition of silver in comparison to peptides **1 – 4** and peptides **S1 – S4**. The band at 222 nm for peptide **4c⁺n⁺** is more negative compared with **4n⁺**, and the band at 208 is approximately the same for both peptides post addition of silver. Both peptides show an increased tendency towards alpha-helicity (**graph 3 and 4**).

3.3.2.1 Circular dichroism over time

Based upon the most significant results from CD analysis, we decided to perform measurements of **AC** and **4c⁺** over 5 days.

A slight change can be seen between days 0 and 5 on the CD spectra for **AC** (**graph 5**). At day 5, the bands at 193 nm and 208 nm increase slightly becoming more positive, whereas at 222 nm, the band decreases slightly becoming more negative. At day 0, the peptide shows a greater tendency towards alpha-helicity in comparison to day 5.
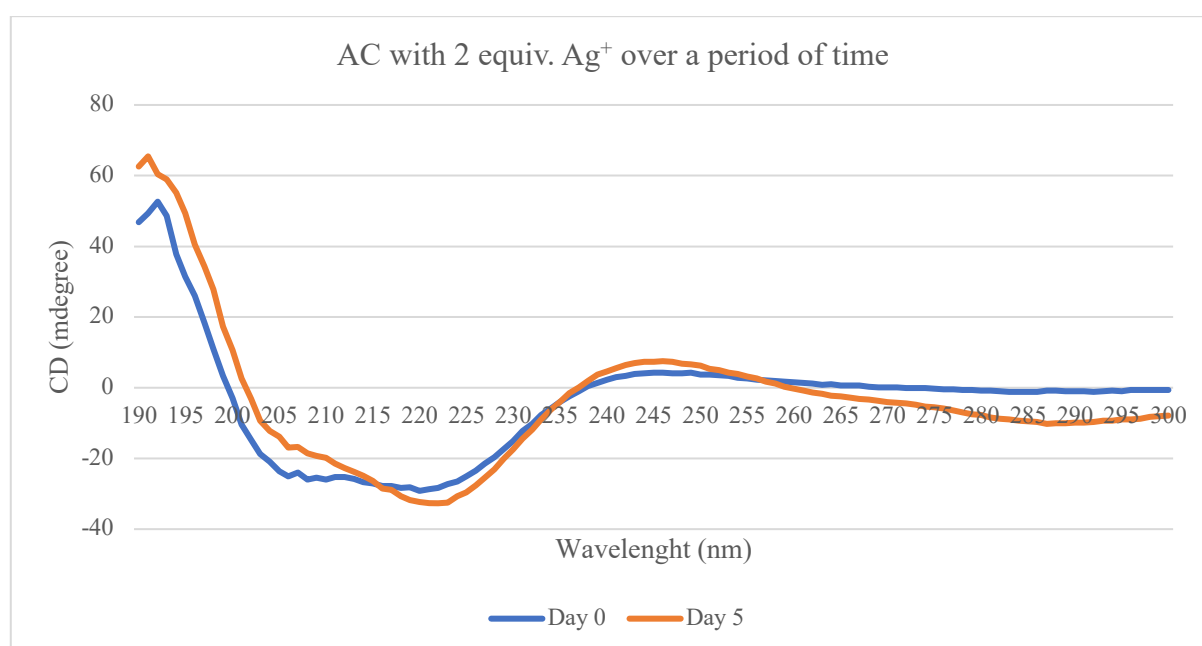
Graph 5: CD spectra for AC 2 equiv. Ag⁺ over a 5-day period

*The graph shows the CD spectra recorded for peptide **AC** with the addition of 2 equiv. Ag⁺ over a period. The blue curve indicates the measurement taken on day 0, and the orange curve indicates the measurements taken on day 5. The x-axis shows the wavelength in nm and the y-axis show the CD in mdegree.*

A major change can be seen between days 0 and 5 on the CD spectra for **4c⁺** (**graph 6**). At day 5, the bands at 193 nm and 208 nm decrease becoming more negative, whereas the band at 222 nm shows

no major change. Furthermore, the peptide shows a greater tendency towards a random-coil secondary structure in comparison to day 0.
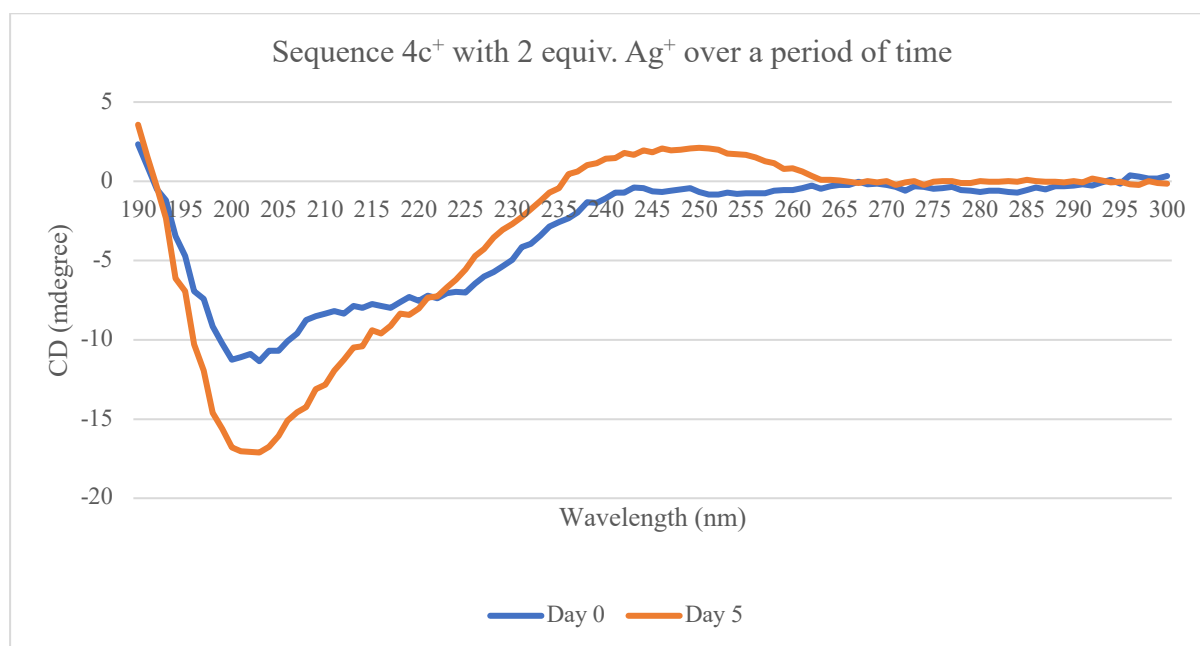
Graph 6: CD spectra for 4c⁺ with 2 equiv. Ag⁺ over a 5-day period

*The graph shows the CD spectra recorded for peptide **4c⁺** with the addition of 2 equiv. Ag⁺ over a period. The blue curve indicates the measurement taken on day 0, and the orange curve indicates the measurements taken on day 5. The x-axis shows the wavelength in nm and the y-axis show the CD in mdegree.*

3.4 Biological assays

3.4.1   Minimum inhibitory concentration

All compounds were tested for their antimicrobial activity against SA. The results obtained from the MIC-assays can be seen in **table 13**. Two MIC-assays were performed in parallel to each other using two different ON cultures. Furthermore, each peptide was tested in duplicates. The MIC-value was read as the lowest concentration of peptide showing no visible bacterial growth. Overall, all peptides with Ag^+-addition show a better MIC-value (i.e., better potential) in comparison to the peptides without Ag^+-addition.

Regarding peptides **1 – 4**, better MIC-values for these peptides were expected, as they have been tested before and their MIC-values are documented in the literature. According to literature, peptide **1** had a MIC-value of >200 µg/mL, peptide **2** had a MIC-value of 50 µg/mL, peptide **3** had a MIC-value of 25 µg/mL and peptide **4** had a MIC-value of 3.1 µg/mL. Besides peptide **1**, the MIC-values recorded in the literature are lower than those obtained during our experiment[11].

For peptides **S1 – S4** without Ag^+-addition, no inhibition was expected, which corresponds to the results obtained during our experiment. The results for **S1 – S4** with Ag^+-addition showed a better MIC-value (i.e., better potential) in comparison to the peptides (**S1 – S4**) without Ag^+-addition.

Ag^+ exhibited great potency due to its low MIC-value (0.745 µg/mL). Furthermore, **AC** without Ag^+-addition showed no inhibition. On the other hand, **AC** with Ag^+-addition showed inhibition at 33.25 µg/mL, which was not expected. During our experiment, Polymyxin B and Melittin were used as positive controls and both antibiotics showed activity. Our MIC-value for Melittin was 8.31 µg/mL, whereas the MIC-value recorded in literature was 3.1 µg/mL[11]. Moreover, the MIC-value for Polymyxin B against SA (GP) was 133 µg/mL, which could be explained by Polymyxin B being an antibiotic normally used against GN bacteria[86].

Table 13: Overview of MIC replicates and MIC results

*The table shows two to four different replicates of the MIC experiment, which were carried out on all our peptides including peptides used as controls (**AC** and **ENDO**) and two known antibiotics (Melittin and Polymyxin B). The MIC-values for each peptide were determined based on the lowest concentration with no visible bacterial growth. Values assigned as ">133" indicate that the peptides precise MIC-value could not be determined as they were above our tested concentration range.*

Peptide name	ON 1 MIC 1.1 [$\mu g/mL$]	ON 2 MIC 1.2 [$\mu g/mL$]	ON 3 MIC 2.1 [$\mu g/mL$]	ON 4 MIC 2.2 [$\mu g/mL$]
1	>133	>133	>133	>133
1 w. Ag^+	2.08	2.08	2.08	2.08
2	>133	>133	>133	>133
2 w. Ag^+	8.31	8.31	8.31	8.31
3	>133	>133	>133	>133
3 w. Ag^+	4.15	4.15	8.31	4.15
4	>133	>133	>133	>133
4 w. Ag^+	8.31	8.31	8.31	8.31
S1	>133	>133	>133	>133
S1 w. Ag^+	2.08	2.08	4.15	2.08
S2	>133	>133	>133	>133
S2 w. Ag^+	2.08	2.08	2.08	2.08
S3	>133	>133	>133	>133
S3 w. Ag^+	2.08	2.08	2.08	2.08
S4	>133	>133	>133	>133
S4 w. Ag^+	2.08	2.08	2.08	4.15
$4c^+$	>133	>133	>133	>133
$4c^+$ w. Ag^+	2.08	2.08	2.08	2.08
$4n^+$	133	133	133	133
$4n^+$ w. Ag^+	2.08	2.08	2.08	2.08
$4c^+n^+$	>133	>133	>133	>133
$4c^+n^+$ w. Ag^+	8.31	4.15	8.31	4.15
AC	>133	>133		
AC w. Ag^+	33.25	33.25		
Polymyxin B	133	133		
ENDO	>133	>133		
Melittin	16.25	8.31		
Pure Ag^+	0.745	0.745	0.745	0.745

3.4.1.1 Spot test

To investigate whether the peptide concentrations were bactericidal or bacteriostatic, a spot-test was performed from the MIC wells. Peptide concentrations were assigned as being bacteriostatic if there was visible bacterial growth after incubation at 37 °C for 18 hours, whereas they were assigned as bactericidal if there was no bacterial growth after incubation at 37 °C for 18 hours.

The results showed that 8 peptide concentrations were assigned as being bacteriostatic at the lowest concentration tested (1st concentration), whereas only two concentrations were bacteriostatic at the two-fold higher concentration (2nd concentration). Based on these results, it was observed that some peptides became bactericidal at the concentration above the MIC-value (**table 14**).

Table 14: Spot test results

The table shows the peptides at two different concentrations, where the 1st concentration is equalled to the MIC-value, and the 2nd concentration is 2-fold higher than the concentration of the MIC-value. Furthermore, the table shows whether the peptide concentration can be classified as bacteriostatic or bactericidal. A peptide concentration was classified as being bacteriostatic if there was no visible growth on the agar plate after incubation at 37 °C for 18 hours, whereas a peptide concentration is classified as bactericidal if there was visible growth.

Peptide name	MIC [$\mu g/mL$]	1st concentration [$\mu g/mL$]	Assignment	2nd concentration [$\mu g/mL$]	Assignment
1 w. Ag^+	2.08	2.08	Bacteriostatic	4.15	Bacteriostatic
2 w. Ag^+	8.31	8.31	Bacteriostatic	16.63	Bactericidal
3 w. Ag^+	4.15	4.15	Bacteriostatic	8.31	Bactericidal
4 w. Ag^+	8.31	8.31	Bacteriostatic	16.63	Bactericidal
S1 w. Ag^+	2.08	2.08	Bactericidal	4.15	Bactericidal
S2 w. Ag^+	2.08	2.08	Bactericidal	4.15	Bactericidal
S3 w. Ag^+	2.08	2.08	Bactericidal	4.15	Bactericidal
S4 w. Ag^+	2.08	2.08	Bacteriostatic	4.15	Bactericidal
4n$^+$	133	133	Bacteriostatic	133	Bacteriostatic
4n$^+$ w. Ag^+	2.08	2.08	Bactericidal	4.15	Bactericidal
4c$^+$ w. Ag^+	2.08	2.08	Bactericidal	4.15	Bactericidal
4c$^+$n$^+$ w. Ag^+	4.15	4.15	Bacteriostatic	8.31	Bactericidal
AC w. Ag^+	33.25	33.25	Bactericidal	66.5	Bactericidal
Pure Ag^+	0.745	0.745	Bacteriostatic	1.49	Bactericidal

3.4.2 Biofilm

To investigate if the compounds had anti-biofilm effects, a biofilm assay were performed. All experiments were performed four times (which equals to four replicates) and each peptide concentration was tested in technical triplicates on each plate (**section 2.5.2**).

Raw data at OD_{595} was collected from the plate-reader and baseline-correction for all samples and our reference (consisting of pure media and bacteria) was performed manually in Excel. A mean was calculated for each of the technical triplicates, and likewise, a mean was calculated for our reference for every plate. Afterwards, the mean value for each technical replicate was compared to the mean value of the reference on that specific plate. This was done to find the yield of biofilm formation for each sample and for each plate.

An outlier-test was performed for each individual peptide concentration comparing the yield of biofilm formation for all four replicates. Two outliers were found, and these values were disregarded.

A paired T-test was performed to investigate whether there was a significant difference between the reference and the treated samples. Two samples were significantly different, and remainder were non-significantly (NS) different.

The first significant sample was peptide **1** w. Ag^+ with a concentration of 2.08 µg/mL and a corresponding p-value of 0.0363, which indicates a significant difference in comparison to the reference. Furthermore, the mean value for the concentration at 2.08 µg/mL is higher than the reference, which indicates that this concentration encourages biofilm formation. The second significant sample was pure Ag^+ with a concentration of 1.49 µg/mL. The p-value for the concentration at 1.49 µg/mL is 0.0275, indicating a significant difference in comparison to the reference. Furthermore, the mean value for the concentration at 1.49 µg/mL is lower, which indicates that this concentration discourages biofilm formation.

The results have been illustrated graphically for each peptide (**figure 14**) and the remaining statistical data can be found in the appendices (**appendices figure 74**).
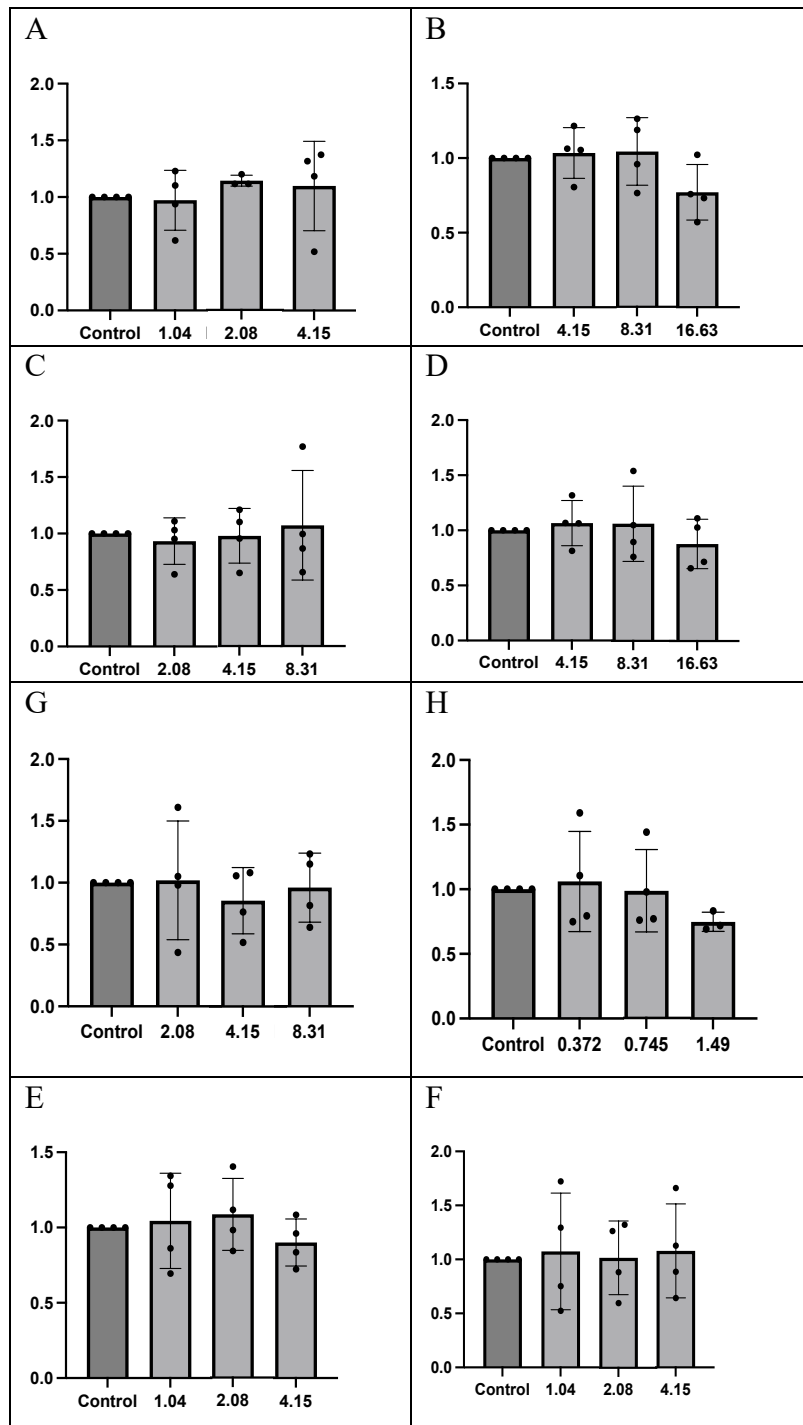
Figure 14: Graphical presentation of biofilm results.

The individual graph shows the reference and the three different concentrations for each given peptide illustrated with dark grey or light grey boxes, respectively. The mean values for each peptide concentration and the reference are illustrated through the height of the boxes. The dots illustrate the individual yield for each replicate. The whiskers illustrate the standard deviation (SD) of differences according to the mean value. The graphs were prepared with Prism. A: Peptide 1 w. Ag^+. B: Peptide 2 w. Ag^+. C: Peptide 3 w. Ag^+. D: Peptide 4 w. Ag^+. E: peptide 4c$^+$ w. Ag^+. F: Peptide 4n$^+$ w. Ag^+. G: peptide 4c$^+$n $^+$ w. Ag^+. H: pure Ag^+.

3.4.3 Haemolysis

To investigate toxicity toward eukaryotic cells a haemolysis assay was conducted by incubating human RBCs with seven different peptides and lysis was measured using a spectrophotometer. Based on the values obtained at OD_{546}, it is possible to calculate the percentage of haemolysis by using **equation 3**:

$$\text{Percentage of haemolysis} = 100 \text{ x } \left(\frac{A_{546 \text{ peptid}} - A_{546 \text{ blank}}}{A_{546 \text{ triton x}-100} - A_{546 \text{ blank}}}\right)$$

Equation 3[81,82]

The percentage of haemolysis for each peptide at their three different concentrations can be seen in **table 15**. A paired t-test was performed to determine whether there was a significant difference between replicate 1 and replicate 2, and the results showed no significant difference. Likewise, a paired t-test was performed between the replicates in comparison to Triton X-100, which showed a significant difference (**table 15**). Based on the t-test, we can conclude the peptides are less toxic than Triton X-100. Other studies have stated that a percentage of haemolysis above 2 % is considered toxic[87,88].

Peptide **4n⁺** w. Ag⁺ at a concentration of 4.15μg/mL and peptide **4c⁺n⁺** w. Ag⁺ at a concentration of 8.31μg/mL have a percentage of haemolysis at 2.2 % and 2.1 %, respectively. These results could suggest that the peptides with the given concentrations could be toxic, however, the deviation is very small.

All the other peptides (**table 15**) do not exhibit haemolytic activity above 2 %, which indicates that they should not be toxic in the tested concentration range. Yet their behaviour at higher concentrations is unknown, as this has not been tested.

Table 15: Haemolytic activity results

*The table shows the different peptides that were selected for the haemolysis assay and the selection was based on the results obtained from the MIC-assay. All peptides were tested in replicates at three different concentrations, where the highest concentration corresponds to a concentration that is 2-fold higher than the MIC-value and the lowest concentration corresponds to a concentration that is 2-fold lower than the MIC-value. The concentration in between corresponds to the MIC-value. The haemolytic activity was calculated in percentage (%) based on **equation 3**.*

Peptide name	Concentration [$\mu g/mL$]	Haemolytic activity (%)	
		Replicate 1	Replicate 2
1 w. Ag$^+$	4.15	0.983	0.791
	2.08	0.623	0.628
	1.04	0.291	0.737
2 w. Ag$^+$	16.63	0.983	1.447
	8.31	0.346	0.791
	4.15	0.318	0.791
3 w. Ag$^+$	8.31	1.010	0.955
	4.15	0.484	1.064
	2.08	0.374	0.573
4 w. Ag$^+$	16.63	0.900	0.737
	8.31	0.401	1.010
	4.15	0.318	0.955
4c$^+$ w. Ag$^+$	4.15	1.204	1.283
	2.08	0.429	0.846
	1.04	0.208	0.846
4n$^+$ w. Ag$^+$	4.15	2.234	1.484
	2.08	1.401	0.748
	1.04	1.068	0.702
4c$^+$n$^+$ w. Ag$^+$	8.31	2.123	1.714
	4.15	1.512	1.254
	2.08	1.013	0.932

4. DISCUSSION

4.1 Determination of the degree of alpha helicity based on CD measurements

As previously mentioned, peptides **1** – **4** did not exhibit any prominent conformational changes post addition of Ag+ (**appendices figure 43 - 46**). However, the results did suggest that a small conformational change has taken place and that the peptides exhibit an alpha-helical tendency.

A reason behind the small observed conformational changes of peptides **1** – **4** could be the length of the peptides (each consisting of 11 AAs). Previously, the shorter peptide **AC** consisting of 6 AAs and an *N*-terminal acetyl group has been shown to adopt alpha-helicity in response to Ag^+-binding, which was also reproduced as a control experiment during the CD measurements. However, when incorporating the slightly modified sequence CAAXC (where X = H or K) into longer peptides, opposing conformational tendencies from the flanking AAs might decrease the willingness of alpha helix induction. Therefore, it cannot be excluded that Ag^+ has been bound to peptides **1** – **4**, but its effect may not have been sufficient to form a prominent alpha-helical conformational change in comparison to **AC**.

Peptide **AC** exhibits a prominent conformational change post addition of Ag^+, however, this peptide stands out for a couple of reasons. Firstly, **AC** only consists of 6 AA, and secondly, it has an acetyl-group in its *N*-terminus, which neutralises the charge, thus increases the alpha-helical dipole moment[89–91].

As expected, peptides **1S** – **4S** did not exhibit any conformational change post addition of Ag^+ due to the lack of cysteine-units which participate in forming an alpha-helical secondary structure. For peptides **4n⁺**, **4c⁺** and **4c⁺n⁺**, the conformational changes post addition of Ag^+ were more prominent especially for peptide **4c⁺**. This may be due to the additional positive charge from the arginine unit in the *C*-terminus, which normally has a positive influence on alpha-helicity, whereas an additional positive charge in the *N*-terminus has the opposite effect. This tendency can be seen for peptide **4c⁺** and **4n⁺**. For **4c⁺n⁺**, the effect of the positive charges in both *C* and *N*-termini have an overall positive effect on alpha-helicity. On that basis, the additional charge in the *C*-terminus of the peptide must have a greater influence on its structure in comparison to an additional charge in the *N*-terminus[89].

For the CD-experiment over several days, it was observed that the secondary structure for peptide **4c$^+$** had changed to a random coiled conformation at day 5 despite the prominent structural changes at day 0. This could indicate that the effect of the Ag$^+$-bond has repealed, and a type of unfavourable "slow reorganisation" has occurred. The "slow reorganisation" may be due to how the peptide solution was stored during the experiment. During the period from day 0 to day 5, the peptide solution was stored at room temperature (19 °C) in a dark drawer with access to oxygen. The access to oxygen could have prompted the formation of disulphide-bridges within the peptide and this could have been verified either using the DTDP method or LC-MS. To prevent this from occurring in future experiments, the peptide solutions could be stored at -20 °C in an air-tight container, or refrigerated between 2 – 8 °C, which is recommended for antibiotics[92]. This tendency has not been observed for peptide **AC**, where the opposite seems to have happened. Once again, this could be due to its shorter length or the addition of the acetyl-group in its *N*-terminus.

4.2 MIC-values and their significance

As a starting point, the peptides with Ag$^+$-addition seem effective regarding their antimicrobial activity as their MIC-values do not exceed 8.31 µg/mL. Due to the large difference in MIC-values for the peptides with and without the addition of Ag$^+$, the results strongly suggest that the addition of Ag$^+$ has had a positive effect on the activity of the peptides. This is consistent with the notion behind the binding-theory between silver and sulphur atoms which promotes alpha-helicity (**section 1.3**). However, it must be considered that Ag$^+$-itself is highly antimicrobial (MIC-value: 0.745 µg/mL), which could be a plausible explanation for the low MIC-values (**table 13**).

This argument contradicts the whole notion behind the binding-theory between Ag$^+$ and sulphur atoms, which has been investigated in other studies[12], and moreover, the theory may not be applicable to other peptides – or at least the peptides investigated in this thesis.

On the other hand, there are multiple indications suggesting that Ag$^+$ is not the only factor involved in killing the bacteria, and that a complex formation between the peptide and Ag$^+$ has occurred. This can be seen when comparing the results investigating the MIC-value for Ag$^+$ only with the concentration of Ag$^+$ within each peptide sample.

Table 16: Comparison between MIC-values for peptides 1 – 4 w. Ag+ and Ag+ only

The table shows the MIC-values for Ag+ only, peptides 1 – 4 w. Ag+ alongside the Ag+ concentration within each peptide sample. The concentrations highlighted in green correspond to the MIC-value together with the Ag+ concentration within the given sample. Furthermore, the concentrations highlighted in grey indicate the difference in Ag+ concentration within the sample compared to the MIC-value of Ag+ only.

Ag+ only	1 w. Ag+		2 w. Ag+		3 w. Ag+		4 w. Ag+	
MIC (µg/mL)	MIC (peptide µg/mL)	Ag+ concentration within sample (µg/mL)	MIC (peptide µg/mL)	Ag+ concentration within sample (µg/mL)	MIC (peptide µg/mL)	Ag+ concentration within sample (µg/mL)	MIC (peptide µg/mL)	Ag+ concentration within sample (µg/mL)
190.83	133	133.25	133	83.25	133	190	133	108.25
95.41	66.5	66.62	66.5	41.62	66.5	95	66.5	54.12
47.70	33.25	33.31	33.25	20.81	33.25	47.5	33.25	27.06
23.70	16.63	16.65	16.63	10.40	16.63	23.75	16.63	13.53
11.92	8.31	8.32	8.31	5.20	8.31	11.87	8.31	6.76
5.96	4.15	4.16	4.15	2.60	4.15	5.93	4.15	3.38
2.98	2.08	2.08	2.08	1.30	2.08	2.96	2.08	1.69
1.49	1.04	1.04	1.04	0.65	1.04	1.48	1.04	0.84
0.745								
0.3725								
0.186								
0.093								

When looking at peptide **1** w. Ag+, the MIC-value was 2.08 µg/mL, which also corresponds to a concentration of 2.08 µg/mL Ag+ within the sample. If unbound Ag+-ions killed the bacteria alone, we would have expected a MIC-value around 1.04 µg/mL, which corresponds to a concentration of 1.04 µg/mL Ag+ within the sample, i.e., an Ag+ concentration that is closer to the MIC-value of Ag+ only. The tendency seen for peptide **1** has also been observed for peptides **2**, **3** and **4**, where the concentration of Ag+ within the sample is too high in comparison to the MIC-value of Ag+ only within the sample.

This strongly suggests that the formation of a complex between Ag+ and the peptide has occurred, since Ag+ is more potent unbound, which cannot be seen in the results for peptide **1 – 4** w. Ag+ (**table 16**).

From a different perspective, the MIC-values can be seen as descriptors of the peptides' ability to inhibit Ag+ activity. To some extent, the MIC-values can describe the binding affinity of Ag+ to the peptides; the greater the difference between the concentrations of Ag+ added to peptide sample compared to the MIC-value of Ag+ only. On that basis, the peptide with the best binding affinity for

Ag$^+$ out of peptides **1** – **4** w. Ag$^+$ appears to be peptides **2** and **4** (both w. Ag$^+$), as the difference between the Ag$^+$-concentrations within each sample is the greatest in comparison to the MIC-value of Ag$^+$ only, and furthermore, they have the highest MIC-values.

However, it is unbeknown how big a role the two different factors contribute towards the MIC-value, so the exact effect of free Ag$^+$ and the Ag$^+$ peptide complex within the sample is not known.

Table 17: Comparison between MIC-values for peptides 1S – 4S w. Ag$^+$ and Ag$^+$ only

*The table shows the MIC-values for Ag$^+$ only, peptides **1S** – **4S** w. Ag$^+$ alongside the Ag$^+$ concentration within each peptide sample. The concentrations highlighted in green correspond to the MIC-value together with the Ag$^+$ concentration within the given sample. Furthermore, the concentrations highlighted in grey indicate the difference in Ag$^+$ concentration within the sample compared to the MIC-value of Ag$^+$ only. In the case of peptides **1S** – **4S** w. Ag$^+$, there is no difference between the Ag$^+$ concentration within each sample compared to the MIC-value of Ag$^+$ only.*

Ag$^+$ only	1S w. Ag$^+$		2S w. Ag$^+$		3S w. Ag$^+$		4S w. Ag$^+$	
MIC (µg/mL)	MIC (peptide µg/mL)	Ag$^+$ concentration within sample (µg/mL)	MIC (peptide µg/mL)	Ag$^+$ concentration within sample (µg/mL)	MIC (peptide µg/mL)	Ag$^+$ concentration within sample (µg/mL)	MIC (peptide µg/mL)	Ag$^+$ concentration within sample (µg/mL)
190.83	133	52.5	133	52.5	133	55	133	57.5
95.41	66.5	26.25	66.5	26.25	66.5	27.5	66.5	28.75
47.70	33.25	13.12	33.25	13.12	33.25	13.75	33.25	14.37
23.70	16.63	6.56	16.63	6.56	16.63	6.87	16.63	7.18
11.92	8.31	3.28	8.31	3.28	8.31	3.43	8.31	3.59
5.96	4.15	1.64	4.15	1.64	4.15	1.71	4.15	1.79
2.98	2.08	0.82	2.08	0.82	2.08	0.85	2.08	0.89
1.49	1.04	0.41	1.04	0.41	1.04	0.42	1.04	0.44
0.745								
0.3725								
0.186								
0.093								

For peptides **1S** – **4S** w. Ag$^+$, we did not expect to see any difference between the MIC-values for the samples with and without Ag$^+$ added, since these peptides do not have cysteine units within their sequences (**table 17**). Cysteine units are required for the formation of an Ag$^+$-peptide complex. However, we saw a significant difference between the samples with and without Ag$^+$; there was a drastic decrease in MIC-value as soon as Ag$^+$ was added to the samples. Upon looking at the concentration of Ag$^+$ within each sample, we can see that peptides **1S** – **4S** w. Ag$^+$ exhibit the opposite tendency in comparison to peptides **1** – **4** w. Ag$^+$.

Peptides **1S** and **2S** both had a MIC-value at 2.08 µg/mL (0.82 µg/mL Ag^+ added to the sample), and the concentration of Ag^+ within these samples resemble the MIC-value of Ag^+ only the most. Furthermore, for peptides **3S** and **4S**, the MIC-values were 2.08 µg/mL (0.85 µg/mL Ag^+ added to the sample) and 2.08 µg/mL (0.89 µg/mL Ag^+ added to the sample), respectively (**table 17**). Therefore, the activity of Ag^+ does not seem to be inhibited, which indicates that there has been no formation of a complex between the peptides and Ag^+, and that the low MIC-values are due to the presence of free Ag^+. Furthermore, this is in agreement with the results obtained during the CD-experiment, where no change was observed following the addition of Ag^+.

Table 18: Comparison between MIC-values for peptides 4C+ w. Ag+, 4N+ w. Ag+, 4C+N+ w. Ag+, AC w. Ag+ and Ag+ only

*The table shows the MIC-values for Ag^+ only, peptides **4C+** w. Ag+, **4N+** w. Ag+, **4C+N+** w. Ag^+, AC w. Ag^+ alongside the Ag^+ concentration within each peptide sample. The concentrations highlighted in green correspond to the MIC-value together with the Ag^+ concentration within the given sample. Furthermore, the concentrations highlighted in grey indicate the difference in Ag^+ concentration within the sample compared to the MIC-value of Ag^+ only.*

Ag^+ only	4C+ w. Ag^+		4N+ w. Ag^+		4C+N+ w. Ag^+		AC w. Ag^+	
MIC (µg/mL)	MIC (peptide µg/mL)	Ag^+ concentration within sample (µg/mL)	MIC (peptide µg/mL)	Ag^+ concentration within sample (µg/mL)	MIC (peptide µg/mL)	Ag^+ concentration within sample (µg/mL)	MIC (peptide µg/mL)	Ag^+ concentration within sample (µg/mL)
190.83	133	70.5	133	150	133	70.5	133	67.5
95.41	66.5	35.25	66.5	75	66.5	35.25	66.5	33.75
47.70	33.25	17.62	33.25	37.5	33.25	17.62	33.25	16.87
23.70	16.63	8.81	16.63	18.75	16.63	8.81	16.63	8.43
11.92	8.31	4.40	8.31	9.37	8.31	4.40	8.31	4.21
5.96	4.15	2.2	4.15	4.68	4.15	2.2	4.15	2.10
2.98	2.08	1.10	2.08	2.34	2.08	1.10	2.08	1.05
1.49	1.04	0.55	1.04	1.17	1.04	0.55	1.04	0.52
0.745								
0.3725								
0.186								
0.093								

For peptides **4n+** w. Ag^+ and **4c+n+** w. Ag^+, the MIC-values were 2.08 µg/mL (2.34 µg/mL Ag^+ added to the sample) and 4.15 µg/mL (2.30 µg/mL Ag^+ added to the sample), respectively (**table 18**). These MIC-values and Ag^+-concentrations should have been lower if the killing of bacteria was due to the presence of free Ag^+. However, peptide **4c+** w. Ag^+ had a MIC-value of 2.08 µg/mL (1.10 µg/mL Ag^+ added to the sample), which strongly suggests that there is a presence of unbound Ag^+, since the concentration of Ag^+ within the sample corresponds closely to the MIC-value of Ag^+ only (**table 18**).

For peptide AC, a similar trend has been observed for peptides **1 – 4** w. Ag$^+$. The MIC-value for **AC** was 33.25 µg/mL (16.87 µg/mL Ag$^+$ added to the sample). The Ag$^+$-concentration within the sample is much higher than the MIC-value for Ag$^+$ only, which suggests the formation of a complex between Ag$^+$ and peptide, but the extent is unknown (**table 18**).

However, it is important to keep in mind that there was a large difference in the results from the CD-experiment with and without Ag$^+$ for the peptides **4c$^+$**, **4n$^+$**, **4c$^+$n$^+$** and **AC**. Due to these results, the low MIC-values could also suggest that it is the complex itself, that is responsible for the MIC-value and not the presence of free Ag$^+$. On the other hand, the results from the CD-experiment for peptides **1 – 4** suggest a combination of complex and the presence of free Ag$^+$, as no major changes were observed on the CD-spectra[1,2,31].

To investigate the precise MIC-value for the complex alone, the peptide solution should have been purified further, where the excess of free Ag$^+$ and possibly unbound peptide would have been removed. The removal of these could have led to a more accurate MIC-result for the individual peptides, as it is currently not possible to conclude what proportion of the MIC-value is due to the presence of Ag$^+$ or complex.

Purification of the peptide complexes could potentially have been carried out using the preparatory HPLC. This would have been possible for peptide AC, where the difference in retention time of the peptide with and without Ag$^+$-addition was significant (**appendices figure 29**) whereas it is unknown whether this technique would function for the longer sequences, as the retention time does not change drastically, which was seen for peptide 4 with and without Ag$^+$-addition (**appendices figure 28**). Therefore, the separation of complex and free peptide might not be possible for all peptides using this technique.

To remove free Ag$^+$ from within the samples, EDTA could be used as it is a chelating agent that captures free metals, such as Ag$^+$. The elimination of free Ag$^+$ would have given more accurate MIC-results[93,94]. However, it must also be considered that EDTA can affect the bacterial cell walls due to its chelating properties. Therefore, it would be necessary to remove EDTA through further purification before any biological experiments[95].

4.3 Potentially renewed relevance of the resistance problem

Throughout this thesis, we have assumed that there was no free Ag^+ present within our solutions. This has been based on previous studies[12] coupled with theory on HSAB-interactions, where the Ag^+-bond to sulphur should form a strong covalent bond. However, several indications are pointing towards this not being the case. One possibility could be that the bonding of Ag^+ to sulphur does not occur fully. A second possibility could be that the bond breaks over time, in which case the resistance problem becomes relevant again.

If there is a large amount of free Ag^+ present within the peptide solution, or if the peptides undergo slow reorganisation, several aspects must be reconsidered concerning the biology to proceed any further. As mentioned earlier, the development of Ag^+-resistance is already prevalent. To avoid the dangers of the development of resistance towards current forms of treatment containing Ag^+, there is a need for further studies on the Ag^+-bond and its durability.

If this is not done, there is a risk that the fight against resistant bacteria will become even more challenging to overcome in future. Therefore, it is not beneficial that the peptide complex has potential as a future treatment if it worsens present treatments unless the negative factor, in this case, excess Ag^+, is removed from the solution.

4.4 Future potential for the peptides

Despite the ambiguous results obtained during the MIC-assay, all results from the biofilm assay indicate that there were no significant changes in the biofilm formation upon addition of Ag^+ to the peptides. On the first hand, this can be considered unfortunate, as new antimicrobial agents to combat the formation of biofilms are in the spotlight, but on the other hand, it can be considered positive as the peptides do not promote the formation of biofilm either.

Additionally, when executing the experiment, it was observed that the SA biofilm was very porous, and this aspect must also be taken into consideration. The outcome could have looked different, if the experiment had been repeated even more, and if a different and hardier bacterium had been selected.

Alongside the results obtained from the biofilm experiment, the peptides have also been shown not to be toxic towards human RBC, which is a sign of potential as a future antimicrobial agent. However,

experiments performed on other cell types would be crucial to ensure that the peptides do not exhibit toxicity against these.

Generally, the haemolytic activity increases in line with the hydrophobicity[96], and since the peptides investigated during this thesis are relatively hydrophilic, this gives rise to the possibility to development of the sequences further.

However, it must still be considered that the haemolytic activity was only investigated around the MIC-value for each peptide. It is therefore unknown, if the peptides become toxic at higher concentrations, as all substances become toxic at some point.

Furthermore, AMPs generally have a severe problem regarding their haemolytic effect[3], which is normally high (toxic). In comparison to other studies, no haemolytic effect was observed below a peptide concentration of 200 µg/mL, and therefore we can assume that the same must be true to some extent for our peptides.

CONCLUSION & FUTURE OUTLOOK

The antimicrobial activity of AMPs is dependent on several different factors, which must be accommodated to increase their activities. The aim of this thesis was to investigate whether the antimicrobial activity of the derivatives based on the alpha-helical region within Tenecin 1 against SA would improve following the addition of Ag^+.

Moreover, if the addition of Ag^+ had a stabilising effect on the alpha-helical region of the peptide sequences. Based on the results, it can be concluded that the S-Ag^+-bond was formed to some extent within all the peptides, where especially peptides **4c⁺**, **4c⁺n⁺** and **AC** showed greater structural changes following the addition of Ag^+ in comparison to the other peptides. Through this thesis, it has been shown that binding of Ag^+ occurs in other peptides besides the model peptide **AC**, and that the number of positive charges and their position within the peptide had a positive effect in relation to promoting alpha-helical structure.

However, it is difficult to conclude to which effect the binding of Ag^+ had regarding activity, as it must be assumed that free Ag^+-ions have influenced the results regarding antimicrobial activity. In summary, the binding of Ag^+ has contributed to increase the activity, but the extent is unknown. Furthermore, it can be concluded that the addition of Ag^+ had no effect on SA biofilm, however, the results also showed that the peptides with Ag^+ were non-toxic towards human RBC. On that basis, the peptides with Ag^+ exhibit potential for further modifications and optimisation and could potentially be used as therapeutic drugs in future.

The modification of peptides could include optimisation of the antimicrobial activity through AA substitution, an increase of positive charges or the addition of an acetyl in the *N*-terminus, which can contribute to increased stability of the peptide. Furthermore, it has been shown that *N*-terminal and/or *C*-terminal modification increases the biological half-life of peptides thus decreasing the rate of proteolytic degradation[1,91]. Another possible way to optimise the peptides is by replacing the cysteine units with histidine units as Ag^+-ions also bind to the imidazole within the histidine unit[97,98].

In addition, an optimised procedure such as automation of the synthesis process could improve the speed, accuracy, and reproducibility of the peptide synthesis, and purification of the peptide to remove free Ag^+-ions.

5. EXPERIMENTAL PROCEDURES

General remarks

The chemicals were acquired from commercial providers and used as received. All solvents were either of HPLC or peptide synthesis quality.

Analytical HPLC Analytical HPLC measurements were recorded by using an Agilent HP1100 instrument with an XBridge® column (10 μm, 4.6 x 100 mm) using a linear gradient of acetonitrile (CAN) in water with 0.1 % TFA. The gradient ran from 0 % to 90 % MeCN over a period of 10 minutes with a flow rate of 1.0 mL/min (method A). Peaks were measured by UV absorption at 215, 230, and 254 nm[12].

Preparative HPLC Purification of peptides was performed by using a Gilson 215 semi-preparative HPLC-system with an XTerra® preperatory column (10 μm, 19 x 150 mm) with a flow rate of 15 mL/min. Detection was performed by measurement of absorbance of UV light at 220 and 280 nm using a Gilson UV/Vis-155 Dual Wavelength Detector (DWD). For the mobile phase, two buffers were used: buffer A (0.1 % TFA in water) and buffer B (0.1 % TFA in 9:1 MeCN/water)[12].

CD measurements were performed by using a Jasco J-715 spectropolarimeter with a constant pressure of 60 bar and a room temperature of 19 °C. The measurements were performed using a 1 mm cuvette, and each sample was scanned three times. Each spectrum was recorded in the range of 300 – 190 nm with a scanning speed of 50 nm/min, a response time of 1 second, and bandwidth of 1.0 nm. Data obtained from each scan was analysed using the software Spectra Manager, version 1.53.01.

UV-VIS measurements were obtained by using a Shimadzu UV-2600 UV-Vis spectrophotometer, with a doublet beam and analysed using the software UVProbe. The measurements were performed using a 1 cm cuvette and the spectra were recorded in the range of 600 – 200 nm.

^{1}H NMR spectra were recorded on a Bruker ADVANCE III HD 400 NB spectrometer with a PA BBO 400S1 BBF-H-D-05 Z SP probe. Chemical shift values are quoted in ppm. ^{1}H spectra and ^{19}F spectra were obtained with the frequencies of 400.131 MHz and 376.460 MHz, respectively. D_2O (4.79 ppm), H_2O (4.79 ppm) and DMSO (2.50 ppm) were used as solvents in different samples and water suppression were used, furthermore, TMS was used as an intern reference (0.0 ppm).

LC-MS spectra were recorded on a Dionex UltiMate 300 instrument (Thermo scientific) with an Acclaim™ RSLC 120 C_{18} column (with the following measurements: 2.2 μm, 120Å, 2.1 x 100 mm), the instrument was coupled to a Bruker microTOF-QIII mass spectrometer. The detection was performed by measurement of absorbance of UV light at 214, 225, 250 and 275 nm. The method was a gradient method, with a start concentration of 4.5 % MeCN/water with 0.1 % formic acid and a final concentration of 90 %MeCN/water with 0.1 % formic acid. The method took 8 minutes to run and had a flowrate of 0.5mL/min[12].

5.1 Chemical synthesis – SPPS

All peptides were synthesised manually via SPPS in filtration columns equipped with polyethylene frits manually. A fluoren-9-ylmethyloxycarbonyl (Fmoc) strategy was used for SPPS. The resin of choice was the Fmoc- Rink Amide AM resin. All AAs and resin were acquired through Chem-impex (Wood Dale, Illinois, USA).

5.1.1 Synthesis of peptide 1 (DAACAAHCLWR) on solid phase

Preparation of resin: The peptides were prepared by SPPS using a dry Fmoc-Rink amide resin (0.4g, loading 0.94 mmol/g). The resin was transferred to a column containing a polyethylene filter at the bottom. Firstly, the resin was saturated in DMF and set to rest for a few minutes.

To remove the Fmoc protecting group on the resin: Once the resin had doubled in size, it was treated with a mixture of piperidine (20 % in DMF) and set to rest for two minutes. Treatment of the resin with piperidine was repeated once again and set to rest for 18 minutes. The column was flushed in between and after the two treatments with piperidine. The resin was then washed once with DMF, twice with CH_2Cl_2 and three times with DMF.

Coupling of amino acids to the resin: The *C*-terminal AA Fmoc-Arg (Pbf)-OH (MW: 648.8 g/mol, 731,8 mg, 3 equiv.), TBTU (MW: 321.1 g/mol, 362.2 mg, 3 equiv.) and DIPEA (MW: 129.25 g/mol, 262 µL) were dissolved in approximate 1 mL DMF. After 5 minutes the solution was added to column containing the resin and set to rest for two hours at room temperature.

The column was flushed, and the resin was washed once with DMF, twice with CH_2Cl_2 and three times with DMF. Treatment with piperidine was repeated twice following the same procedure as described above. The resin was then washed once with DMF, twice with CH_2Cl_2 and three times with DMF. All the steps were repeated with the following AAs until the desired peptide was synthesised: Fmoc-Trp(Boc)-OH (MW: 526.6 g/mol, 594 mg, 3 equiv.), Fmoc-Leu-OH (MW: 353.4 g/mol, 398.6 mg, 3 equiv.), Fmoc-Cys(Trt)-OH (MW: 585.7 g/mol, 660.7 mg, 3 equiv.), Fmoc-His(Trt)-OH (MW: 619.6 g/mol, 698.9 mg, 3 equiv.), Fmoc-Ala-OH (MW: 311.3 g/mol, 351.1 mg, 3 equiv.), Fmoc-Ala-OH (MW: 311.3 g/mol, 351.1 mg, 3 equiv.), Fmoc-Cys(Trt)-OH (MW: 585.7 g/mol, 660.7 mg, 3 equiv.), Fmoc-Ala-OH (MW: 311.3 g/mol, 351.1 mg, 3 equiv.), Fmoc-Ala-OH (MW: 311.3 g/mol, 351.1 mg, 3 equiv.), Fmoc-Asp(OtBu)-OH (MW: 411.5 g/mol, 464.2 mg, 3 equiv.).

To cleave off the peptide from the resin: When the desired peptide was obtained, the resin was then washed once with DMF, twice with CH$_2$Cl$_2$ and three times with DMF. Additionally, the resin was washed tree times with CH$_2$Cl$_2$. Reagent B (88 % TFA/5 % H$_2$O/5 % phenol/2 % tri-isopropyl silane (TIPS)) was added to the column top and set to rest for 3 hours. The TFA phase was then collected and concentrated by evaporation by a flow of N$_2$ to remove the TFA. The evaporated liquid was then dissolved in 10 % MeCN and the phenol was removed by using diethyl ether, where the water phase was collected for further work (Analytical HPLC, preparatory HPLC, and LC-MS) and the desired fraction from the preparatory HPLC was later freeze-dried for 3 days.

5.1.2 Synthesis of peptide 2 (KAACAAHCLWR) on solid phase

The same procedure as described in **section 5.1.1** was repeated with the following AAs until the desired peptide was synthesised: Fmoc-Arg(Pbf)-OH (MW: 648.8 g/mol, 731,8 mg, 3 equiv.), Fmoc-Trp(Boc)-OH (MW: 526.6 g/mol, 594 mg, 3 equiv.), Fmoc-Leu-OH (MW: 353.4 g/mol, 398.6 mg, 3 equiv.), Fmoc-Cys(Trt)-OH (MW: 585.7 g/mol, 660.7 mg, 3 equiv.), Fmoc-His(Trt)-OH (MW: 619.6 g/mol, 698.9 mg, 3 equiv.), Fmoc-Ala-OH (MW: 311.3 g/mol, 351.1 mg, 3 equiv.), Fmoc-Ala-OH (MW: 311.3 g/mol, 351.1 mg, 3 equiv.), Fmoc-Cys(Trt)-OH (MW: 585.7 g/mol, 660.7 mg, 3 equiv.), Fmoc-Ala-OH (MW: 311.3 g/mol, 351.1 mg, 3 equiv.), Fmoc-Ala-OH (MW: 311.3 g/mol, 351.1 mg, 3 equiv.), Fmoc-Lys(Boc)-OH (MW: 468.5 g/mol, 528.5 mg, 3 equiv.).

5.1.3 Synthesis of peptide 3 (DAACAAKCLWR) on solid phase

The same procedure as described in **section 5.1.1** was repeated with the following AAs until the desired peptide was synthesised: Fmoc-Arg(Pbf)-OH (MW: 648.8 g/mol, 731,8 mg, 3 equiv.), Fmoc-Trp(Boc)-OH (MW: 526.6 g/mol, 594 mg, 3 equiv.), Fmoc-Leu-OH (MW: 353.4 g/mol, 398.6 mg, 3 equiv.), Fmoc-Cys(Trt)-OH (MW: 585.7 g/mol, 660.7 mg, 3 equiv.), Fmoc, Lys(Boc)-OH (MW: 468.5 g/mol, 528.5 mg, 3 equiv.), Fmoc-Ala-OH (MW: 311.3 g/mol, 351.1 mg, 3 equiv.), Fmoc-Ala-OH (MW: 311.3 g/mol, 351.1 mg, 3 equiv.), Fmoc-Cys(Trt)-OH (MW: 585.7 g/mol, 660.7 mg, 3 equiv.), Fmoc-Ala-OH (MW: 311.3 g/mol, 351.1 mg, 3 equiv.), Fmoc-Ala-OH (MW: 311.3 g/mol, 351.1 mg, 3 equiv.), Fmoc-Asp(OtBu)-OH (411.5 g/mol, 464.2 mg, 3 equiv.).

5.1.4 Synthesis of peptide 4 (KAACAAKCLWR) on solid phase

The same procedure as described in **section 5.1.1** was repeated with the following AAs until the desired peptide was synthesised: Fmoc-Arg(Pbf)-OH (MW: 648.8 g/mol, 731,8 mg, 3 equiv.), Fmoc-Trp(Boc)-OH (MW: 526.6 g/mol, 594 mg, 3 equiv.), Fmoc-Leu-OH (MW: 353.4 g/mol, 398.6 mg, 3 equiv.), Fmoc-Cys(Trt)-OH (MW: 585.7 g/mol, 660.7 mg, 3 equiv.), Fmoc-Lys(Boc)-OH (MW: 468.5 g/mol, 528.5 mg, 3 equiv.), Fmoc-Ala-OH (MW: 311.3 g/mol, 351.1 mg, 3 equiv.), Fmoc-Ala-OH (MW: 311.3 g/mol, 351.1 mg, 3 equiv.), Fmoc-Cys(Trt)-OH (MW: 585.7 g/mol, 660.7 mg, 3 equiv.), Fmoc-Ala-OH (MW: 311.3 g/mol, 351.1 mg, 3 equiv.), Fmoc-Ala-OH (MW: 311.3 g/mol, 351.1 mg, 3 equiv.), Fmoc-Lys(Boc)-OH (MW: 468.5 g/mol, 528.5 mg, 3 equiv.).

5.1.5 Synthesis of peptide S1 (DAASAAHSLWR) on solid phase

The same procedure as described in **section 5.1.1** was repeated with the following AAs until the desired peptide was synthesised: Fmoc-Arg(Pbf)-OH (MW: 648.8 g/mol, 731,8 mg, 3 equiv.), Fmoc-Trp(Boc)-OH (MW: 526.6 g/mol, 594 mg, 3 equiv.), Fmoc-Leu-OH (MW: 353.4 g/mol, 398.6 mg, 3 equiv.), Fmoc-Ser(tBu)-OH (MW: 383.4 g/mol, 432.5 mg, 3 equiv.), Fmoc-His(Trt)-OH (MW: 619.6 g/mol, 698.9 mg, 3 equiv.), Fmoc-Ala-OH (MW: 311.3 g/mol, 351.1 mg, 3 equiv.), Fmoc-Ala-OH (MW: 311.3 g/mol, 351.1 mg, 3 equiv.), Fmoc-Ser(tBu)-OH (MW: 383.4 g/mol, 432.5 mg, 3 equiv.), Fmoc-Ala-OH (MW: 311.3 g/mol, 351.1 mg, 3 equiv.), Fmoc-Ala-OH (MW: 311.3 g/mol, 351.1 mg, 3 equiv.), Fmoc-Asp(OtBu)-OH (MW: 411.5 g/mol, 464.2, 3 equiv.).

5.1.6 Synthesis of peptide S2 (KAASAAHSLWR) on solid phase

The same procedure as described in **section 5.1.1** was repeated with the following AAs until the desired peptide was synthesised: Fmoc-Arg(Pbf)-OH (MW: 648.8 g/mol, 731,8 mg, 3 equiv.), Fmoc-Trp(Boc)-OH (MW: 526.6 g/mol, 594 mg, 3 equiv.), Fmoc-Leu-OH (MW: 353.4 g/mol, 398.6 mg, 3 equiv.), Fmoc-Ser(tBu)-OH (MW: 383.4 g/mol, 432.5 mg, 3 equiv.), Fmoc-His(Trt)-OH (MW: 619.6 g/mol, 698.9 mg, 3 equiv.), Fmoc-Ala-OH (MW: 311.3 g/mol, 351.1 mg, 3 equiv.), Fmoc-Ala-OH (MW: 311.3 g/mol, 351.1 mg, 3 equiv.), Fmoc-Ser(tBu)-OH (MW: 383.4 g/mol, 432.5 mg, 3 equiv.), Fmoc-Ala-OH (MW: 311.3 g/mol, 351.1 mg, 3 equiv.), Fmoc-Ala-OH (MW: 311.3 g/mol, 351.1 mg, 3 equiv.), Fmoc-Lys(Boc)-OH (MW: 468.5 g/mol, 528.5 mg, 3 equiv.).

5.1.7 Synthesis of peptide S3 (DAASAAKSLWR) on solid phase

The same procedure as described in **section 5.1.1** was repeated with the following AAs until the desired peptide was synthesised: Fmoc-Arg(Pbf)-OH (MW: 648.8 g/mol, 731,8 mg, 3 equiv.), Fmoc-Trp(Boc)-OH (MW: 526.6 g/mol, 594 mg, 3 equiv.), Fmoc-Leu-OH (MW: 353.4 g/mol, 398.6 mg, 3 equiv.), Fmoc-Ser(tBu)-OH (MW: 383.4 g/mol, 432.5 mg, 3 equiv.), Fmoc-Lys(Boc)-OH (MW: 468.5 g/mol, 528.5 mg, 3 equiv.), Fmoc-Ala-OH (MW: 311.3 g/mol, 351.1 mg, 3 equiv.), Fmoc-Ala-OH (MW: 311.3 g/mol, 351.1 mg, 3 equiv.), Fmoc-Ser(tBu)-OH (MW: 383.4 g/mol, 432.5 mg, 3 equiv.), Fmoc-Ala-OH (MW: 311.3 g/mol, 351.1 mg, 3 equiv.), Fmoc-Ala-OH (MW: 311.3 g/mol, 351.1 mg, 3 equiv.), Fmoc-Asp(OtBu)-OH (MW: 411.5 g/mol, 464.2 mg, 3 equiv.).

5.1.8 Synthesis of peptide S4 (KAASAAKSLWR) on solid phase

The same procedure as described in **section 5.1.1** was repeated with the following AAs until the desired peptide was synthesised: Fmoc-Arg(Pbf)-OH (MW: 648.8 g/mol, 731,8 mg, 3 equiv.), Fmoc-Trp(Boc)-OH (MW: 526.6 g/mol, 594 mg, 3 equiv.), Fmoc-Leu-OH (MW: 353.4 g/mol, 398.6 mg, 3 equiv.), Fmoc-Ser(tBu)-OH (MW: 383.4 g/mol, 432.5 mg, 3 equiv.), Fmoc-Lys(Boc)-OH (MW: 468.5 g/mol, 528.5 mg, 3 equiv.), Fmoc-Ala-OH (MW: 311.3 g/mol, 351.1 mg, 3 equiv.), Fmoc-Ala-OH (MW: 311.3 g/mol, 351.1 mg, 3 equiv.), Fmoc-Ser(tBu)-OH (MW: 383.4 g/mol, 432.5 mg, 3 equiv.), Fmoc-Ala-OH (MW: 311.3 g/mol, 351.1 mg, 3 equiv.), Fmoc-Ala-OH (MW: 311.3 g/mol, 351.1 mg, 3 equiv.), Fmoc-Lys(Boc)-OH (MW: 468.5 g/mol, 528.5 mg, 3 equiv.).

5.1.9 Synthesis of peptide 4c⁺ (KAACAAKCLWRR) on solid phase

The same procedure as described in **section 5.1.1** was repeated with the following AAs until the desired peptide was synthesised: Fmoc-Arg(Pbf)-OH (MW: 648.8 g/mol, 731,8 mg, 3 equiv.), Fmoc-Arg(Pbf)-OH (MW: 648.8 g/mol, 731,8 mg, 3 equiv.), Fmoc-Trp(Boc)-OH (MW: 526.6 g/mol, 594 mg, 3 equiv.), Fmoc-Leu-OH (MW: 353.4 g/mol, 398.6 mg, 3 equiv.), Fmoc-Cys(Trt)-OH (MW: 585.7 g/mol, 660.7 mg, 3 equiv.), Fmoc-Lys(Boc)-OH (MW: 468.5 g/mol, 528.5 mg, 3 equiv.), Fmoc-Ala-OH (MW: 311.3 g/mol, 351.1 mg, 3 equiv.), Fmoc-Ala-OH (MW: 311.3 g/mol, 351.1 mg, 3 equiv.), Fmoc-Cys(Trt)-OH (MW: 585.7 g/mol, 660.7 mg, 3 equiv.), Fmoc-Ala-OH (MW: 311.3 g/mol, 351.1 mg, 3 equiv.), Fmoc-Ala-OH (MW: 311.3 g/mol, 351.1 mg, 3 equiv.), Fmoc-Lys(Boc)-OH (MW: 468.5 g/mol, 528.5 mg, 3 equiv.).

5.1.10 Synthesis of peptide 4n⁺ (RKAACAAKCLWR) on solid phase

The same procedure as described in **section 5.1.1** was repeated with the following AAs until the desired peptide was synthesised: Fmoc-Arg(Pbf)-OH (MW: 648.8 g/mol, 731,8 mg, 3 equiv.), Fmoc-Trp(Boc)-OH (MW: 526.6 g/mol, 594 mg, 3 equiv.), Fmoc-Leu-OH (MW: 353.4 g/mol, 398.6 mg, 3 equiv.), Fmoc-Cys(Trt)-OH (MW: 585.7 g/mol, 660.7 mg, 3 equiv.), Fmoc-Lys(Boc)-OH (MW: 468.5 g/mol, 528.5 mg, 3 equiv.), Fmoc-Ala-OH (MW: 311.3 g/mol, 351.1 mg, 3 equiv.), Fmoc-Ala-OH (MW: 311.3 g/mol, 351.1 mg, 3 equiv.), Fmoc-Cys(Trt)-OH (MW: 585.7 g/mol, 660.7 mg, 3 equiv.) , Fmoc-Ala-OH (MW: 311.3 g/mol, 351.1 mg, 3 equiv.), Fmoc-Ala-OH (MW: 311.3 g/mol, 351.1 mg, 3 equiv.), Fmoc-Lys(Boc)-OH (MW: 468.5 g/mol, 528.5 mg, 3 equiv.), Fmoc-Arg(Pbf)-OH (MW: 648.8 g/mol, 731,8 mg, 3 equiv.).

5.1.11 Synthesis of peptide 4c⁺n⁺ (RKAACAAKCLWRR) on solid phase

The same procedure as described in **section 5.1.1** was repeated with the following AAs until the desired peptide was synthesised: Fmoc-Arg(Pbf)-OH (MW: 648.8 g/mol, 731,8 mg, 3 equiv.), Fmoc-Arg(Pbf)-OH (MW: 648.8 g/mol, 731,8 mg, 3 equiv.), Fmoc-Trp(Boc)-OH (MW: 526.6 g/mol, 594 mg, 3 equiv.), Fmoc-Leu-OH (MW: 353.4 g/mol, 398.6 mg, 3 equiv.), Fmoc-Cys(Trt)-OH (MW: 585.7 g/mol, 660.7 mg, 3 equiv.), Fmoc-Lys(Boc)-OH (MW: 468.5 g/mol, 528.5 mg, 3 equiv.), Fmoc-Ala-OH (MW: 311.3 g/mol, 351.1 mg, 3 equiv.), Fmoc-Ala-OH (MW: 311.3 g/mol, 351.1 mg, 3 equiv.), Fmoc-Cys(Trt)-OH (MW: 585.7 g/mol, 660.7 mg, 3 equiv.), Fmoc-Ala-OH (MW: 311.3 g/mol, 351.1 mg, 3 equiv.), Fmoc-Ala-OH (MW: 311.3 g/mol, 351.1 mg, 3 equiv.), Fmoc-Lys(Boc)-OH (MW: 468.5 g/mol, 528.5 mg, 3 equiv.), Fmoc-Arg(Pbf)-OH (MW: 648.8 g/mol, 731,8 mg, 3 equiv.)

5.1.12 Synthesis of peptide ENDO (YPWF) on solid phase

The same procedure as described in **section 5.1.1** was repeated with the following AAs until the desired peptide was synthesised: Fmoc-Phe-OH (MW: 387.4 g/mol, 437 mg, 3 equiv.)**,** Fmoc-Trp(Boc)-OH (MW: 526.6 g/mol, 594 mg, 3 equiv.), Fmoc-Pro-OH (MW: 337.4 g/mol, 380.6 mg, 3 equiv.), Fmoc-Tyr(tBu)-OH (MW: 459 g/mol, 518 mg, 3 equiv.).

5.1.13 Synthesis of peptide AC (AC – RCAAAC) on solid phase

The same procedure as described in **section 5.1.1** was repeated with the following AAs until the desired peptide was synthesised: Fmoc-Cys(Trt)-OH (MW: 585.7 g/mol, 660.7 mg, 3 equiv.), Fmoc-Ala-OH (MW: 311.3 g/mol, 351.1 mg, 3 equiv.), Fmoc-Ala-OH (MW: 311.3 g/mol, 351.1 mg, 3 equiv.), Fmoc-Ala-OH (MW: 311.3 g/mol, 351.1 mg, 3 equiv.), Fmoc-Cys(Trt)-OH (MW: 585.7 g/mol, 660.7 mg, 3 equiv.), Fmoc-Arg(Pbf)-OH (MW: 648.8 g/mol, 731,8 mg, 3 equiv.). Lastly, acetic acid (MW: 60.05 g/mol, 64.48 µL, 3 equiv.) was connected to the peptide using the same procedure.

REFERENCES

1. Kang, S. J., Kim, D. H., Mishig-Ochir, T. & Lee, B. J. Antimicrobial peptides: Their physicochemical properties and therapeutic application. *Archives of Pharmacal Research* vol. 35 409–413. doi.org/10.1007/s12272-012-0302-9 (2012).

2. Li, J. *et al.* Membrane active antimicrobial peptides: Translating mechanistic insights to design. *Frontiers in Neuroscience* vol. 11. doi.org/10.3389/fnins.2017.00073 (2017).

3. Lei, J. *et al.* The antimicrobial peptides and their potential clinical applications. *Am J Transl Res* vol. 11 3919–3931. ISSN: 1943-8141/AJTR0095989 (2019).

4. Browne, K. *et al.* A new era of antibiotics: The clinical potential of antimicrobial peptides. *International Journal of Molecular Sciences* vol. 21 1–23. doi.org/10.3390/ijms21197047 (2020).

5. Schmidtchen, A., Pasupuleti, M. & Malmsten, M. Effect of hydrophobic modifications in antimicrobial peptides. *Advances in Colloid and Interface Science* vol. 205 265–274. doi.org/10.1016/j.cis.2013.06.009 (2014).

6. Appelbaum, P. C. The emergence of vancomycin-intermediate and vancomycin-resistant Staphylococcus aureus. *Clinical Microbiology and Infection* vol. 12 16–23. doi.org/10.1111/j.1469-0691.2006.01344.x (2006).

7. CDC. *Antibiotic resistance threats in the United States, 2019.* doi:10.15620/cdc:82532. (2019)

8. Nguyen, L. T., Haney, E. F. & Vogel, H. J. The expanding scope of antimicrobial peptide structures and their modes of action. *Trends in Biotechnology* vol. 29 464–472. doi.org/10.1016/j.tibtech.2011.05.001 (2011).

9. Mahlapuu, M., Håkansson, J., Ringstad, L. & Björn, C. Antimicrobial peptides: An emerging category of therapeutic agents. *Frontiers in Cellular and Infection Microbiology* vol. 6. doi.org/10.3389/fcimb.2016.00194 (2016).

10. Giangaspero, A., Sandri, L. & Tossi, A. Amphipathic α helical antimicrobial peptides: A systematic study of the effects of structural and physical properties on biological activity. *European Journal of Biochemistry* vol. 268 5589–5600. doi.org/10.1046/j.1432-1033.2001.02494.x (2001).

11. Ahn, H. S. *et al.* Design and synthesis of novel antimicrobial peptides on the basis of α helical domain of Tenecin 1, an insect defensin protein, and structure-activity relationship study. *Peptides* vol. 27 640–648. doi.org/10.1016/j.peptides.2005.08.016 (2006).

12.   Fischer, N. H. PhD thesis Cysteine-selective peptide stapling and protein labeling. 183–246 (2022). ISBN 978-87-93732-35-3.

13.   Mijnendonckx, K., Leys, N., Mahillon, J., Silver, S. & Van Houdt, R. Antimicrobial silver: Uses, toxicity and potential for resistance. *BioMetals* vol. 26 609–621. doi.org/10.1007/s10534-013-9645-z (2013).

14.   Kim, J. S. *et al.* Antimicrobial effects of silver nanoparticles. *Nanomedicine: Nanotechnology, Biology, and Medicine* vol. 3 95–101. doi.org/10.1016/j.nano.2006.12.001 (2007).

15.   Lu, J. *et al.* Both silver ions and silver nanoparticles facilitate the horizontal transfer of plasmid-mediated antibiotic resistance genes. *Water Research* vol. 169. doi.org/10.1016/j.watres.2019.115229 (2020).

16.   Hadrup, N., Sharma, A. K. & Loeschner, K. Toxicity of silver ions, metallic silver, and silver nanoparticle materials after in vivo dermal and mucosal surface exposure: A review. *Regulatory Toxicology and Pharmacology* vol. 98 257–267. doi.org/10.1016/j.yrtph.2018.08.007 (2018).

17.   Hadrup, N. & Lam, H. R. Oral toxicity of silver ions, silver nanoparticles and colloidal silver - A review. *Regulatory Toxicology and Pharmacology* vol. 68 1–7. doi.org/10.1016/j.yrtph.2013.11.002 (2014).

18.   L. Nelson, D. & M. Cox, M. 3. Amino Acids, Peptides, And peptides. in *Lehninger Principles of biochemistry* 75–114 (W.H Freeman and Company, 2017).

19.   L. Nelson, D. & M. Cox, M. 4. The three-Dimensional structure of proteins. in *Lehninger Principles of biochemistry* 115–156 (W.H Freeman and Company, 2017).

20.   M. Cox, M., A. Doudna, J. & O'Donnell, M. 4. Protein Structure. in *Molecular Biology, principles and practice* 93–132 (W. H. Freeman and Company, 2015).

21.   Griffith, E. C. & Vaida, V. In situ observation of peptide bond formation at the water-air interface. *PNAS* vol. 109. doi.org/10.1073/pnas.1210029109 (2012).

22.   Hol, W. G. J. THE ROLE OF THE ALPHA-HELIX DIPOLE IN PROTEIN FUNCTION AND STRUCTURE. *prog. Biophys. Molec. Biol* vol. 45 149–195 (1985).

23.   Schiffer, M. & Edmundson, A. B. Use of Helical Wheels to Represent the Structures of Proteins and to Identify Segments with Helical Potential. *Biophysical Journal* vol. 7 121–135. doi.org/10.1016/S0006-3495(67)86579-2 (1967).

24.   Jenssen, H., Hamill, P. & Hancock, R. E. W. Peptide antimicrobial agents. *Clinical Microbiology Reviews* vol. 19 491–511. doi.org/10.1128/CMR.00056-05 (2006).

25. Fjell, C. D., Hiss, J. A., Hancock, R. E. W. & Schneider, G. Designing antimicrobial peptides: Form follows function. *Nature Reviews Drug Discovery* vol. 11 37–51. doi.org/10.1038/nrd3591 (2012).

26. Havkic, E., Brasch Palme, I., Paludan Larsen, J. & Maagaard Hansen, S. *Cyclization and lipid tale addition of derivatives from the antimicrobial peptide indolicidin concerning approvement of antibacterial activity*. (2021).

27. Hancock, R. E. W. & Sahl, H. G. Antimicrobial and host-defense peptides as new anti-infective therapeutic strategies. *Nature Biotechnology* vol. 24 1551–1557. doi.org/10.1038/nbt1267 (2006).

28. Huan, Y., Kong, Q., Mou, H. & Yi, H. Antimicrobial Peptides: Classification, Design, Application and Research Progress in Multiple Fields. *Frontiers in Microbiology* vol. 11. doi.org/10.3389/fmicb.2020.582779 (2020).

29. Willy, J., Sandman, K. & Wood, S. *Prescott's microbiology*. (McGraw-Hill education, 2020).

30. Silhavy, T. J., Kahne, D. & Walker, S. The bacterial cell envelope. *Cold Spring Harbor perspectives in biology* vol. 2. doi.org/10.1101/cshperspect.a000414 (2010).

31. Le, C. F., Fang, C. M. & Sekaran, S. D. Intracellular targeting mechanisms by antimicrobial peptides. *Antimicrobial Agents and Chemotherapy* vol. 61. doi.org/10.1128/AAC.02340-16 (2017).

32. Lee, K. H., Hong, S. Y. & Oh, J. E. Synthesis and structure-function study about tenecin 1, an antibacterial protein from larvae of Tenebrio molitor. *FEBS Letters* vol. 439 41–45. doi.org/10.1016/S0014-5793(98)01333-7 (1998).

33. Ahn, H. sun *et al.* Design and synthesis of cyclic disulfide-bonded antibacterial peptides on the basis of the α helical domain of Tenecin 1, an insect defensin. *Bioorganic and Medicinal Chemistry* vol. 16 4127–4137. doi.org/10.1016/j.bmc.2008.01.019 (2008).

34. Joo Moon, H., Young Lee, S., Kurata, S., Natori, S. & Luel Lee, B. Purification and Molecular Cloning of cDNA for an Inducible Antibacterial Protein from Larvae of the Coleopteran, Tenebrio molitor. *J. Biochem* vol. 116 53–58. doi.org/10.1093/oxfordjournals.jbchem.a124502 (1994).

35. Russell, A. D. & Hugo, W. B. Antimicrobial Activity and Action of Silver. *Progress in Medicinal Chemistry* vol. 31 351–370. doi.org/10.1016/S0079-6468(08)70024-9 (1994).

36. Eckhardt, S. *et al.* Nanobio silver: Its interactions with peptides and bacteria, and its uses in medicine. *Chemical Reviews* vol. 113 4708–4754. doi.org/10.1021/cr300288v (2013).

37. Hosny, A. E. D. M. S., Rasmy, S. A., Aboul-Magd, D. S., Kashef, M. T. & El-Bazza, Z. E. The increasing threat of silver-resistance in clinical isolates from wounds and burns. *Infection and Drug Resistance* vol. 12 1985–2001. doi.org/10.2147/IDR.S209881 (2019).

38. Stabryla, L. M. *et al.* Role of bacterial motility in differential resistance mechanisms of silver nanoparticles and silver ions. *Nature Nanotechnology* vol. 16 996–1003. doi.org/10.1038/s41565-021-00929-w (2021).

39. Feng, Q. L. *et al.* A mechanistic study of the antibacterial effect of silver ions on Escherichia coli and Staphylococcus aureus. *Journal of Biomedical Materials Research* vol. 52 662–668. doi.org/10.1002/1097-4636(20001215)52:4<662::AID-JBM10>3.0.CO;2-3 (2000).

40. Kumar, S. Prediction of Metal Ion Binding Sites in Proteins from Amino Acid Sequences by Using Simplified Amino Acid Alphabets and Random Forest Model. *Genomics & Informatics* vol. 15 162–169. doi.org/10.5808/gi.2017.15.4.162 (2017).

41. Balogh, R. K. *et al.* Flexibility of the CueR Metal Site Probed by Instantaneous Change of Element and Oxidation State from AgI to CdII. *Chemistry - A European Journal* vol. 26 7451–7457. doi.org/10.1002/chem.202000132 (2020).

42. Kelso, M. J. *et al.* α-Turn Mimetics: Short Peptide α-Helices Composed of Cyclic Metallopentapeptide Modules. *Journal of the American Chemical Society* vol. 126 4828–4842. doi.org/10.1021/ja037980i (2004).

43. Vidugiris, G.-J. A., Razumas, V. J., Drungiliene, A. A. & Kulys, J. J. Complex formation of amino acids and proteins with silver ions. *J. Electroanal. Chem., and constituting* vol. 19 513–520. doi.org/10.1016/0302-4598(88)80030-8 (1988).

44. Passerini, A., Punta, M., Ceroni, A., Rost, B. & Frasconi, P. Identifying cysteines and histidines in transition-metal-binding sites using support vector machines and neural networks. *Proteins: Structure, Function and Genetics* vol. 65 305–316. doi.org/10.1002/prot.21135 (2006).

45. Tang, S. & Zheng, J. Antibacterial Activity of Silver Nanoparticles: Structural Effects. *Advanced Healthcare Materials* vol. 7. doi.org/10.1002/adhm.201701503 (2018).

46. G. Sharpe, A. & E. Housecroft, C. Acids, bases and ions in aqueous solution. in *Inorganic chemistry* (Pearson, 2018).

47. Leung, B. O., Jalilehvand, F., Mah, V., Parvez, M. & Wu, Q. Silver(I) complex formation with cysteine, penicillamine, and glutathione. *Inorganic Chemistry* vol. 52 4593–4602. doi.org/10.1021/ic400192c (2013).

48.   Ho, T.-L. The Hard Soft Acids Bases (HSAB) Principle and Organic Chemistry. *Chemical Reviews* vol. 75 (1975).

49.   McMurry, J. Polar covalent bonds; Acids and Bases. in *Organic chemistry with biological applications* 28–31 (Cengage, 2015).

50.   Horsfall, M. & Spiff, A. I. Equilibrium Sorption Study of Al 3+, Co 2+ and Ag+ in Aqueous Solutions by Fluted Pumpkin (Telfairia Occidentalis HOOK f) Waste Biomass. *Acta Chim. Slov* vol. 52 174–181 (2005).

51.   6.15:   periodic   trends   -   atomic   radius.   *LibreTexts* https://chem.libretexts.org/Bookshelves/Introductory_Chemistry/Introductory_Chemistry_(C K-12)/06%3A_The_Periodic_Table/6.15%3A_Periodic_Trends-_Atomic_Radius (2022).

52.   Iwadate, Y., Kawamura, K., Igarashi, K. & Mochinaga, J. Effective Ionic Radii of NO2- and SCN- Estimated in Terms of the Bóttcher Equation and the Lorentz-Lorenz Equation. *J. Phys. Chem* vol. 86 5205–5208 (1982).

53.   E. Housecroft, C. & G. Sharpe, A. Structures and energetics of metallic and ionic solids. in *Inorganic chemistry* 162–164 (Pearson, 2008).

54.   Atomic   Radii.   *LibreTexts* https://chem.libretexts.org/Bookshelves/Physical_and_Theoretical_Chemistry_Textbook_Ma ps/Supplemental_Modules_(Physical_and_Theoretical_Chemistry)/Physical_Properties_of_ Matter/Atomic_and_Molecular_Properties/Atomic_Radii (2023).

55.   Taylor TA & Unakal CG. Staphylococcus Aureus. (*StatsPearls Publishing)* https://www.ncbi.nlm.nih.gov/books/NBK441868/ (2022).

56.   Foster, T. J. Staphylococcus aureus. *Academic Press*. doi.org/10.1006/bkmnl.2001.0039 (2001).

57.   CDC.   Deadly   Staph   Infections   Still   Threaten   the   U.S.   *CDC* https://www.cdc.gov/media/releases/2019/p0305-deadly-staph-infections.html (2019).

58.   SSI. *Staphylococcus aureus bacteraemia Cases in Denmark 2021*. (2021).

59.   Moormeier, D. E. & Bayles, K. W. Staphylococcus aureus biofilm: a complex developmental organism. *Molecular Microbiology* vol. 104 365–376. doi.org/10.1111/mmi.13634 (2017).

60.   Köck, R. *et al.* Methicillin-resistant Staphylococcus aureus (MRSA): burden of disease and control   challenges   in   Europe.   Eurosurveillance   15,   1-9. http://www.eurosurveillance.org/ViewArticle.aspx?ArticleId=19688 (2010).

61. Bhattacharya, M., Wozniak, D. J., Stoodley, P. & Hall-Stoodley, L. Prevention and treatment of Staphylococcus aureus biofilms. *Expert Review of Anti-Infective Therapy* vol. 13 1499–1516. doi.org/10.1586/14787210.2015.1100533 (2015).

62. Preda, V. G. & Săndulescu, O. Communication is the key: biofilms, quorum sensing, formation and prevention. *Discoveries* vol. 7 1–11. doi.org/10.15190/d.2019.13 (2019).

63. López, D., Vlamakis, H. & Kolter, R. Biofilms. *Cold Spring Harbor perspectives in biology* vol. 2. doi.org/10.1101/cshperspect.a000398 (2010).

64. Bogino, P. C., Oliva, M. de las M., Sorroche, F. G. & Giordano, W. The role of bacterial biofilms and surface components in plant-bacterial associations. *International Journal of Molecular Sciences* vol. 14 15838–15859. doi.org/10.3390/ijms140815838 (2013).

65. Periasamy, S. *et al.* How Staphylococcus aureus biofilms develop their characteristic structure. *Proceedings of the National Academy of Sciences of the United States of America* vol. 109 1281–1286. doi.org/10.1073/pnas.1115006109 (2012).

66. Gross, M., Cramton, S. E., Götz, F. & Peschel, A. Key role of teichoic acid net charge in Staphylococcus aureus colonization of artificial surfaces. *Infection and Immunity* vol. 69 3423–3426. doi.org/10.1128/IAI.69.5.3423-3426.2001 (2001).

67. Kaplan, J. B. Antibiotic-induced biofilm formation. *International Journal of Artificial Organs* vol. 34 737–751. doi.org/10.5301/ijao.5000027 (2011).

68. Hargittai, I. Bruce Merrifield centennial: pioneer of chemical synthesis on solid matrix. *Structural Chemistry* vol. 32 2083–2086. doi.org/10.1007/s11224-021-01822-x (2021).

69. Fields, G. B. & Noble, R. L. Solid phase peptide synthesis utilizing 9-fluorenylmethoxycarbonyl amino acids. *Int. J. Peptide Protein Res* vol. 35 161–214 (1990).

70. Orain, D., Ellard, J. & Bradley, M. Protecting groups in solid-phase organic synthesis. *Journal of combinatorial chemistry* vol. 4 1–16. doi.org/10.1021/cc0001093 (2002).

71. Sharma, A. *et al.* Understanding Tetrahydropyranyl as a Protecting Group in Peptide Chemistry. *ChemistryOpen* vol. 6 168–177. doi.org/10.1002/open.201600156 (2017).

72. Luna, O. F. *et al.* Deprotection reagents in Fmoc solid phase peptide synthesis: Moving away from piperidine? *Molecules* vol. 21. doi.org/10.3390/molecules21111542 (2016).

73. Riener, C. K., Kada, G. & Gruber, H. J. Quick measurement of protein sulfhydryls with Ellman's reagent and with 4,4′-dithiodipyridine. *Analytical and Bioanalytical Chemistry* vol. 373 266–276. doi.org/10.1007/s00216-002-1347-2 (2002).

74. How to calculate peptide concentration. *Biosynthesis* https://www.biosyn.com/faq/how-to-calculate-peptide-concentration.aspx (2007).

75. Storage and handling of peptides. *AAPPTEC* https://www.peptide.com/resources/storage-and-handling-of-peptides/ (2022).

76. ATCC. Staphylococcus aureus subsp. aureus Rosenbach. *ATCC* https://www.atcc.org/products/29213 (2022).

77. Kowalska-Krochmal, B. & Dudek-Wicher, R. The Minimum Inhibitory Concentration of Antibiotics: Methods, Interpretation, Clinical Relevance. *Pathogens* vol. 10. doi.org/10.3390/pathogens10020165 (2021).

78. Determination of minimum inhibitory concentrations (MICs) of antibacterial agents by agar dilution. *European Society of Clinical Microbiology and Infection* vol. 6 509–515. doi.org/10.1046/j.1469-0691.2000.00142.x (2000).

79. Wiegand, I., Hilpert, K. & Hancock, R. E. W. Agar and broth dilution methods to determine the minimal inhibitory concentration (MIC) of antimicrobial substances. *Nature Protocols* vol. 3 163–175. doi.org/10.1038/nprot.2007.521 (2008).

80. O'Toole, G. A. Microtiter dish Biofilm formation assay. *Journal of Visualized Experiments*. doi.org/10.3791/2437 (2010).

81. Greco, I. *et al.* Correlation between hemolytic activity, cytotoxicity and systemic in vivo toxicity of synthetic antimicrobial peptides. *Scientific Reports* vol. 10. doi.org/10.1038/s41598-020-69995-9 (2020).

82. Mojsoska, B., Zuckermann, R. N. & Jenssen, H. Structure-activity relationship study of novel peptoids that mimic the structure of antimicrobial peptides. *Antimicrobial Agents and Chemotherapy* vol. 59 4112–4120. doi.org/10.1128/AAC.00237-15 (2015).

83. Huang, Y. *et al.* Role of helicity of α-helical antimicrobial peptides to improve specificity. *Protein and Cell* vol. 5 631–642. doi.org/10.1007/s13238-014-0061-0 (2014).

84. Krause, E., Bienert, M., Schmieder, P. & Wenschuh, H. The helix-destabilizing propensity scale of D-amino acids: The influence of side chain steric effects. *Journal of the American Chemical Society* vol. 122 4865–4870. doi.org/10.1021/ja9940524 (2000).

85. Greenfield, N. J. Using circular dichroism spectra to estimate protein secondary structure. *Nature Protocols* vol. 1 2876–2890. doi.org/10.1038/nprot.2006.202 (2007).

86. Shatri, G. & Tadi, P. Polymyxin. *National library of medicine* https://www.ncbi.nlm.nih.gov/books/NBK557540/ (2022).

87. Lowe, G. *et al.* Nursing Blood Specimen Collection Techniques and Hemolysis Rates in an Emergency Department: Analysis of Venipuncture Versus Intravenous Catheter Collection Techniques. *Journal of Emergency Nursing* vol. 34 26–32. doi.org/10.1016/j.jen.2007.02.006 (2008).

88. Goyal, T. & Schmotzer, C. L. Validation of hemolysis index thresholds optimizes detection of clinically significant hemolysis. *American Journal of Clinical Pathology* vol. 143 579–583. doi.org/10.1309/AJCPDUDE1HRA0YMR (2015).

89. Hol, W. G. J., Van Duijnen, P. T. & Berendsen, H. J. C. The alpha helix dipole and properties of proteins. *Nature* vol. 273 (1978).

90. Peptide Modifications: N-Terminal, Internal, and C-Terminal. *Sigma Aldrich* https://www.sigmaaldrich.com/DK/en/technical-documents/technical-article/protein-biology/protein-labeling-and-modification/peptide-modifications-n-terminal-internal-and-c-terminal

91. Soleymani-Goloujeh, M. *et al.* Effects of N-terminal and C-terminal modification on cytotoxicity and cellular uptake of amphiphilic cell penetrating peptides. *Artificial Cells, Nanomedicine and Biotechnology* vol. 46 91–103. doi.org/10.1080/21691401.2017.1414823 (2018).

92. CareQuality commission. Storing medicines in fridges in care homes. *CareQuality commission* https://www.cqc.org.uk/guidance-providers/adult-social-care/storing-medicines-fridges-care-homes (2022).

93. Oviedo, C. & Rodríguez, J. EDTA: THE CHELATING AGENT UNDER ENVIRONMENTAL SCRUTINY. *Quim. Nova* vol. 26 901–905 (2003).

94. Sigma Aldrich. Chelators. https://www.sigmaaldrich.com/DK/en/technical-documents/technical-article/protein-biology/protein-purification/chelators.

95. Finnegan, S. & Percival, S. L. EDTA: An Antimicrobial and Antibiofilm Agent for Use in Wound Care. *Advances in Wound Care* vol. 4 415–421. doi.org/10.1089/wound.2014.0577 (2015).

96. Chen, Y. *et al.* Role of peptide hydrophobicity in the mechanism of action of α-helical antimicrobial peptides. *Antimicrobial Agents and Chemotherapy* vol. 51 1398–1406. doi.org/10.1128/AAC.00925-06 (2007).

97. Mirolo, L., Schmidt, T., Eckhardt, S., Meuwly, M. & Fromm, K. M. PH-dependent coordination of AgI ions by histidine: Experiment, theory, and a model for SilE. *Chemistry - A European Journal* vol. 19 1754–1761. doi.org/10.1002/chem.201201844 (2013).

98. Guo, Y., Wang, S., Du, H., Chen, X. & Fei, H. Silver Ion-Histidine Interplay Switches Peptide Hydrogel from Antiparallel to Parallel β-Assembly and Enables Controlled Antibacterial Activity. *Biomacromolecules* vol. 20 558–565. doi.org/10.1021/acs.biomac.8b01480 (2019).